PROPOSAL 771
(MAY,1986)

A PROPOSAL TO STUDY BEAUTY PRODUCTION AND OTHER HEAVY QUARK PHYSICS ASSOCIATED WITH DIMUON PRODUCTION IN 800 (925) GEV/C PP INTERACTIONS

M. Arenton, T.Y. Chen, K.W. Lai, N. Yao
University of Arizona

S.E. Anassontzis, S. Katsanevas, C. Kourkoumelis, P. Ioannu, T. Premantiotis, A. Manousakis-Katsikakis, L. K. Resvanis, S. Tzamarias, G. Voulgaris
University of Athens

L. Fortney, A. Goshaw, S. Oh
Duke University

B. Cox, S. Delchamps, C.M. Jenkins, P.O. Mazur, C.T. Murphy, R. Rameika, R. Smith, F. Turkot, W. Yang
Fermilab

D.J. Judd, W.P. Tucker, D.E. Wagoner
Florida A & M University

S. Conetti, M. Haire, A. Marchionni, D. Stairs, L. Turnbull
McGill University

J. Rosen, L. Spiegel
Northwestern University

He Mao, Cheng-Hong Shen, Naijian Zhang, C. Wang
Shandong University

Correspondent:
B. Cox, Fermilab
312-840-3152

I. Introduction

The presence of dimuons in final states produced in hadronic interactions has proved to be a valuable indicator that interesting hard physics processes have taken place. These muon pairs provide a mechanism for selecting these relatively rare processes from interactions due to the total cross section. In particular, processes involving heavy quarks are flagged by the presence of muon pairs. We are proposing to use the high rate E705 spectrometer[1] (shown in Fig. 1) and its dimuon trigger processor[2,3] which have already functioned well in Experiments E-537[4] and E-705 to detect and measure several heavy quark phenomena which result in a final state containing a pair of muons. This experiment will use the primary proton beam from the Tevatron at the maximum energy available at the time of execution of the experiment. The spectrometer will be augmented by the addition of a silicon tracker similar to those[5] used in other experiments at the Fermilab. The present P-West High Intensity Laboratory secondary beam[6] will need to be upgraded by addition of sufficient bending power to allow the transport of the 800 to 925 GeV/c primary proton beam to the experiment target (see Appendix A).

II. Physics Objectives

A) The first goal of this experiment is the measurement of the hadroproduction of beauty in pW interactions using the 800->925 GeV/c primary proton beam from the Tevatron. We will look for beauty mesons, $(B_{\bar{u}})^-$, $(B_{\bar{d}})^0$, $(B_{\bar{s}})^0$, $(B_{\bar{c}})^-$ and their antiparticles produced via

$$pW \longrightarrow \bar{B}\ B + X \qquad (1)$$

where either the B or the $\bar{B}$ decays into

ψ + (anything)$^{\pm}$ (odd number of charged tracks for $B^{\pm}$)
+ (anything)^0 (even number of charged tracks for $B^0, \bar{B}^0$)
$\longrightarrow \mu^+\mu^-$

In addition, we will look for production of beauty baryons such as B_{dd} , B_{uu}

B_{du} , B_{us}, B_{ds} , etc. which can also decay into ψ + anything. Beauty quark baryon production, however, by analogy with light quark baryon production is expected to be considerably less copious than beauty meson production.

The experimental signature for such physics will be events with opposite sign dimuons which point at a secondary decay vertex as measured by the silicon tracker where the muon pairs reconstruct to the ψ mass. The association of the ψ with a secondary decay vertex insures that one is seeing beauty rather than charm production. Since the branching ratio for B —> ψ + anything has been measured by both the ARGUS[7] (1.10±0.19%) and CLEO[8] (1.10±0.21±0.23%) experiments and a rough lifetime for beauty is known ($3.0\pm_1{}^2\times10^{-13}$ sec for the WA75 measurement[9], $1.2\pm0.2\times10^{-12}$ sec for the PEP-PETRA measurements[10,11]), it is possible to determine the cross section for beauty hadroproduction from our observation of associated with secondary vertices without complete reconstruction of the beauty meson final states. The calculation of the cross section without complete reconstruction of particular final states will depend to a small extent on a model dependent estimate of the efficiency for seeing the secondary vertex. Background to the detection of beauty decay comes primarily from "ordinary" ψ production in which the ψ fakes a secondary vertex by reconstructing to a point far from the primary vertex because of measurement errors .

B) In addition to the observation of B —> ψ + anything and the inference of the total cross section for beauty meson production, we intend to reconstruct specific exclusive final states of the beauty mesons containing ψ's. Complete reconstruction of particular exclusive final states permits the direct measurement of momentum and lifetime distributions and provides extra constraints for the measurement of the hadroproduction cross sections for beauty. This complete reconstruction will be possible for some final states. We list in Table I the Cabibbo favored final states for the beauty meson decays which result in less than or equal to three charged particles. Estimated branching ratios[12] are provided in some cases and in one particular case ($B\longrightarrow\psi K^-$) an experimental measurement[13] is available. The antimeson decay table is similar of course except for CP violating effects. We note that the B^0, $\overline{B^0}$ secondary vertices result in an even number of outgoing charged tracks

and the $B^{\pm}$ secondary vertices in an odd number of charged tracks.

Table I

B Meson Decay[+]	Beauty "Mass"	Branching Ratios[12]	Experimental[++] Accessibility
$(B_{\overline{u}})^- \longrightarrow \psi K^-$	$\approx$5.3 GeV/c^2	0.1%	***
		(0.11±0.07%)[13]	
$\psi \overline{K^0} \pi^-$		0.1%	**
$\psi K^- \pi^0$		0.1%	*
$(B_{\overline{d}})^0 \longrightarrow \psi \overline{K^0}$	$\approx$5.3 Gev/c^2	0.1%	**
$\psi K^- \pi^+$		0.1%	***
$\psi \overline{K^0} \pi^0$		0.1%	-
$(B_s)^0 \longrightarrow \psi\psi$	$\approx$5.5 GeV/c^2	0.1%	***
$\psi K^- K^+$	(estimated)	0.1%	***
$\psi K^0 \overline{K^0}$		0.1%	*
$(B_{\overline{c}})^- \longrightarrow \psi D^- K^0$	$\approx$6.7 GeV/c^2	-	
$\psi D^0 K^-$	(estimated)	-	
ψF^-		-	
$\psi \pi^-$		-	***

[+] The $B_{\overline{c}}$ can decay directly to $B_{\overline{u}}$, $B_{\overline{d}}$, $B_{\overline{s}}$ plus anything followed by the subsequent decay of any of the the three B mesons into ψ plus anything. However these decays are more complicated to analyze and are not discussed.

[++] The relative experimental "accessibility" of the final states is roughly indicated by the number of *'s

Most of these relatively simple final states are observable at some level but each has its own special experimental problems. For purposes of the following discussion we will assume no charged K-π identification although we are actively considering implementing such

identification. In the absence of such identification, a K-π ambiguity will be present for all non muon charged tracks. This will necessitate two entries in any $\psi x^- x^+$ or $\psi x^\pm$ mass plot. The final states involving a $\overline{K^0}$ will require the assignment of that $\overline{K^0}$ to the secondary decay vertex without the presence of a charged track in the silicon tracker and will therefore lead to ambiguities between K^0's produced in the secondary vertex and those from the primary vertex. This will increase the spurious mass combinations. For the case of beauty meson final states containing a π^0, all π^0's in the event are candidates for inclusion in the reconstructed secondary vertex. This leads to a large combinatorial background for final states containing a π^0. Considering all of these factors, we have rendered a qualitative judgement about the experimental accessibility of each final state in Table I. Those final states in which the beauty decays result in only charged particles are particularly suited for reconstruction.

C) The third physics goal of this experiment will be the observation of $\overline{B}B$ mixing by observation of high mass, like sign dimuons where each of the muons point to a different secondary vertex. The opposite sign muons from different vertices are due to the semileptonic decays of either charm or beauty and are produced in the process:

$$pW \longrightarrow \overline{B^0}\, B^0 + X \qquad (2)$$
$$\overline{B^0} \hookrightarrow \mu^+ + \nu + \text{anything (odd number of charged tracks)}^-$$
$$B^0 \hookrightarrow \mu^- + \overline{\nu} + \text{anything (odd number of charged tracks)}^+$$

The same sign dimuons of interest are produced when either the $\overline{B^0}$ or the B^0 have evolved into the conjugate antiparticle and produces the same sign muon as its partner in its semileptonic decay.

Backgrounds to the same sign dimuons from $\overline{B}B$ mixing can arise from:

1. The sequential decay of either the B or the $\overline{B}$ into a charmed particle followed by the semi-

leptonic decay of that charmed particle in conjunction with the semileptonic decay of the other B meson. The sign of the lepton produced in the semileptonic decay of the daughter is opposite to the sign of the lepton that would have been produced by the semileptonic decay of the parent thereby leading to a same sign dimuon background.

2. Direct production of and mixing of $C\overline{C}$ pairs (D^0, $\overline{D^0}$ for example) where the charmed particle evolves into the anti-charmed particle and generates a same sign background to the same sign muons from $B^0\overline{B^0}$ mixing.

3. Production of $B\overline{B}$ pairs with one of the B's decaying semileptonically and the other decaying nonleptonically but with one of the pions from the nonleptonic decay undergoing $\pi \longrightarrow \mu\nu$ decay.

The magnitude of these backgrounds and techniques for supressing them are discussed in section VI-C. We will only mention here that these backgrounds can be suppressed since 1)the same sign dimuon signal from $B\overline{B}$ mixing will have higher mass than the same sign dimuon backgrounds and 2)secondary vertices can be identified as beauty decays by their visible mass . We will investigate the effectiveness of these techniques in eliminating same sign backgrounds when the mixing experiment is discussed below.

D) A fourth objective of this experiment will be the continuation at higher energies of the measurement of hadronic production of charmonium which we currently are carrying out at lower energies in Fermilab experiment E-705[1]. We are in the process of measuring

$$\begin{array}{l} \pi^{\pm} \\ p^{\pm} \end{array} N \longrightarrow \chi + \text{anything} \qquad (3)$$
$$\chi \hookrightarrow \gamma\,\psi$$
$$\psi \hookrightarrow \mu^+\mu^-$$

at 300 GeV/c. At the same time as we perform the search for beauty production, we would continue the study of charmonium production at the higher energy using the 800 -> 925 GeV/c primary proton beam to measure χ production from the heavy target:

$$\begin{array}{l} p\,W \longrightarrow \chi + \text{anything} \\ \qquad\quad \hookrightarrow \gamma\,\psi \\ \qquad\qquad\quad \hookrightarrow \mu^+\mu^- \end{array} \qquad (4)$$

The measurement of energy dependence of charmonium production will allow us to more completely determine the production mechanisms and the gluon structure function of the nucleons. (see Ref. 1)

E) Finally, using the primary proton beam at the highest energy we plan to search for evidences of hadronic production of χ_Υ in much the same way that we are measuring charmonium production, i.e.:

$$\begin{array}{l} p\,W \longrightarrow \chi_\Upsilon + \text{anything} \\ \qquad\quad \hookrightarrow \gamma\,\Upsilon \\ \qquad\qquad\quad \hookrightarrow \mu^+\mu^- \end{array} \qquad (5)$$

IV. Beam Requirements/Experiment Running Requirements

We are basing our estimates of yields on a canonical run of 20 weeks of beam. We anticipate **2.8×10^6 seconds of beam** (20 weeks×100 hours/week×60min/hour×23 seconds of spill/min). We will use the primary proton beam to take advantage of the maximum energy available (800—>925 GeV/c). The scheme for the upgrade of the P-West High Intensity Laboratory secondary beam line is straightforward and is detailed in Appendix A. We will require **1.7×10^8 protons per second** of spill or **$\approx3.8\times10^8$ protons per spill** during data taking. This beam intensity implies a total interaction rate of **2×10^6 interactions per second** from our target and our silicon tracker assuming the use of the 700 micron W target described below. Approximately **1×10^6 interactions per second** are generated by each of these devices. We

will trigger only on interactions from the tungsten target by requiring (in the trigger) that there be hits in the first module of the silicon tracker at large angles with respect to the beam. We use the $A^{0.72}$ dependence of the total cross section to predict the silicon and tungsten total cross section and a total inelastic cross section for pN at 800 -> 925 GeV/c of 32×10^{-27} cm^2 per nucleon.

The interaction rate of 2×10^6 interactions per second to be used in P771 (an interaction every 25 buckets or 470 nanoseconds) is the same as that planned for our current experiment, E705, and is an order of magnitude lower than the interaction rate of experiment E537. In our initial run of experiment E705 in the summer of 1985, we operated at an interaction rate of 0.5×10^6 interactions per second with no visible degradation of the spectrometer. Individual parts of the spectrometer such as the electromagnetic calorimeter have been tested in calibration beam at much higher effective rates without degradation. We were limited at the time of our summer 1985 run by an incomplete data acquisition system that was not yet capable of handling and logging 200 events per second. At the present time for E705, we have upgraded our data acquisition system such that it can handle 200 events per second. We have achieved a measured suppression due to our fast dimuon trigger and dimuon trigger processor of 10^{-4} of the raw interaction rate in the summer of 1985.

We will operate in P771 in much the same mode as we intend to operate E705 with the following exceptions: 1) Our beam tagging Cerenkov counters will not be required during data taking. 2) We expect to have a much cleaner trigger situation in P771 because of our use of the extracted proton beam rather than a pion beam with all of its attendant muon halo. 3) By the simple trigger requirement discussed above we will trigger only on interactions from the target and therefore will require our data acquisition system to handle 100 events per second rather than the 200 per second that it is required to handle in E705. 4) We expect to implement some data filtering at the level of our VME based microprocessor event builder to further reduce the requirement on the data acquisition system.

Finally, as in experiment E-705, we will require occasional use of the calibration electron beam for adjustment of our electromagnetic detector. We summarize in Table I below the expected beam usage and the spot sizes that we expect on the experiment target.

Table II

Proton Beam	Max Flux/sec	Flux/spill(23 sec)	σ_x(cm)	σ_y(cm)
800-925 GeV/c	1.7×10^8	3.6×10^9	0.2	0.2

V. Experimental Setup

A) General Remarks

We plan to use the E-705 spectrometer (Figure 1) augmented by a silicon tracker and a W foil target (Figure 2). We will take advantage of the multi-stage dimuon trigger which has been developed for this spectrometer and has already been used in experiment E-537 and is currently being used in experiment E-705. This trigger, which includes an ECL-CAMAC trigger processor[2,3] which forms an dimuon mass in < 10 μs from the muon candidate tracks that it finds in the spectrometer's drift chamber system, presently provides a suppression of $<10^{-4}$ of the interactions due to the total cross section. When this trigger is coupled to our data acquisition system which is capable of handling 200 events/sec, we will operate in P771 at an interaction rate of 2×10^6 interactions per second producing 100 dimuon triggers/second from the target. This is a more comfortable manner of operation than that of E705 which requires that we operate at 200 triggers per second in the absence of filtering.

B) W Foil Target

We have chosen to use a 700 microns thick tungsten foil. Tungsten has been chosen as the target material in spite of the relatively large ratio of interaction length to radiation length for two main reasons:

1. The density of tungsten allows a relatively thin foil for a given number of interaction lengths and minimizes the number of secondary

decay vertices which occur inside the foil and can be confused with interactions of secondaries.

2. The higher A of tungsten optimizes the number of beauty events, relative to a given number of interactions due to the total cross section. The cross section for beauty production is assumed to be linear in A in comparison to the total cross section which increases[21] like $A^{0.72}$.

The total target thickness of 700 microns which we have chosen corresponds to 0.2 radiation lengths and 0.0061 interaction lengths (for protons). We are able to tolerate the relative thinness of the target in interaction lengths because of our use of the extracted proton beam which can easily deliver the required intensity of few $\times 10^8$ protons per second without undue strain on the accelerator.

With this target, if we are limited by our spectrometer to 1×10^6 interactions per second from the target, we can achieve a sensitivity for our canonical run of **375K events per nanobarn** of σ(pN) cross section. We use this number in the calculation of our event yields. Table III below summarizes the parameters of the W foil target that we have chosen for this experiment:

Table III

Target	t_{foil}	#foils	$L(X_0)$	λ^{π}(%)	λ^{p}(%)
W	700μ	1	0.200	0.40	0.61

C) Silicon Tracker

Figure 2 shows the configuration of the silicon tracker that will be used in this experiment. This device consists of three modules, each containing four 300 micron thick silicon planes. The first of these three modules will be 1"×1" and the remaining two modules will be 2"×2". The tracker contains approximately 0.63% of an interaction length and 4% of a radiation length. The modules are spaced by 7 cm as indicated and the tracker is positioned 10000 microns downstream of the W foil in the.

The width of the silicon strips is 50 microns. Because of our relatively thin W target we plan to require in the trigger the presence of wide angle tracks in the first module to insure an interaction in the tungsten. We will do this by the simple expedient of requiring a certain number of hits in the first silicon module outside of the forward direction.

VI. Event Yields/Backgrounds

A) $B\bar{B}$ production in pW interactions at 800—>925 GeV/c

The number of beauty mesons or hadrons that we will observe is uncertain because of the uncertainty in the hadronic production cross sections for beauty. The calculations of Quigg[14], Margolis[15], Combridge[16], Owens[17] and Halzen[18] are shown in Figure 3 along with the current experimental information[11,19] available on beauty hadroproduction. Table IV tabulates the cross sections for 800 and 925 GeV/c pp interactions predicted for some of these calculations. These cross sections have been calculated for a quark mass of 5.3 GeV/c^2. If the appropriate beauty quark mass to use in these calculations is 4.7 GeV/c^2, the cross sections increase by approximately a factor of 2.

Table IV*

Calculation		800 GeV pN	925 GeV pN
Combridge	(Λ=500 MeV)	2.8×10^{-32}	4.6×10^{-32}
Owens	(Λ=400 MeV)	2.1×10^{-32}	3.1×10^{-32}
Owens	(Λ=200 MeV)	9.4×10^{-33}	1.5×10^{-32}
Margolis	($\Lambda\approx$200 MeV)	2.7×10^{-33}	4.1×10^{-33}
Quigg	(Λ=200 MeV)	2.4×10^{-33}	3.8×10^{-33}

* A K factor of two has been multiplied by the QCD cross sections of Combridge, Owens and Quigg to take into account higher order processes[17]. Margolis's calculation has been left as is because of its semi-empirical nature.

Given the target and beam which are described above, Table V shows the number of $B\bar{B}$ events that we expect to produce with the canonical 2.8×10^6 seconds of proton beam at 1.7×10^8 protons/sec **(375K events per 10^{-33} cm^2 of nucleon-nucleon cross section assuming cross sections which vary linearly with A).**

Table V
Number of $B\bar{B}$ Events Produced
In The Canonical Running Time

Calculation		800 GeV pW	925 GeV pW
Combridge	(Λ=500 MeV)	1.1×10^7	1.7×10^7
Owens	(Λ=400 MeV)	8.0×10^6	1.2×10^7
Owens	(Λ=200 MeV)	3.5×10^6	5.6×10^6
Margolis	($\Lambda\approx$200 MeV)	1.0×10^6	1.5×10^6
Quigg	(Λ=200 MeV)	9.0×10^5	1.4×10^6

B) pW $\longrightarrow \bar{B}$ B +anything: $\bar{B}$ (B) $\longrightarrow \psi$ + anything: $\psi \longrightarrow \mu\mu$

Using the model for $B\bar{B}$ production outlined in Appendix B, we calculate acceptances of 25%, and 28% for the two muons resulting from this cascade decay sequence at 800 and 925 GeV/c beam momentum. In calculating the number of B mesons that we will observe decaying into ψ's which subsequently decay into muon pairs, we have used 1.10% (the average of the two existing measurements) for the branching ratio for $B\longrightarrow\psi+x$ and 7% for the branching ratio for the $\psi\longrightarrow\mu^+\mu^-$ decay mode. In addition, we have taken into account the factor of 2 that comes from having both a B and a $\bar{B}$ in the final state. Note that we have also assumed that the branching ratio for $B_u^{\pm}$, B_d^0 , and B_s^0 into ψ plus anything are the same. Under this assumption and the assumption that these three types of B mesons dominate the hadronization of beauty quarks, we can calculate the number of B mesons decays that we expect to see in our canonical run. We tabulate these numbers in Table VI below.

Table VI
Number of B—>ψ + X; ψ—>μμ

Calculation		800 GeV pW	925 GeV pW
Combridge	(Λ=500 MeV)	4240	7330
Owens	(Λ=400 MeV)	3080	5170
Owens	(Λ=200 MeV)	1350	2410
Margolis	(Λ≈200 MeV)	390	650
Quigg	(Λ=200 MeV)	350	600

All of these numbers must be multiplied by an efficiency for surviving the vertex cuts which are necessary to isolate true beauty decays with a clean, unconfused secondary vertex in the silicon tracker and to eliminate false secondary vertices from "ordinary" ψ decays. In addition, all the other usual standard reconstruction efficiencies such as those due to PWC's, drift chambers,etc must be taken into account. We now discuss the identification and reconstruction of the secondary vertices in the B—>ψ—>μμ decays.

We have estimated the resolutions with which a decay vertex can be reconstructed and the efficiency with which it can be separated from the W foil and the other vertices in the event by the use of a Monte Carlo incorporating the B production and decay model of Appendix B (which uses a 0.6 $\times 10^{-12}$ second beauty lifetime). This Monte Carlo incorporates the expected resolution of the silicon tracker and the multiple scattering in the W target and the silicon tracker. The resolution for reconstruction of secondary vertices using only the muon tracks from the ψ is calculated to be:

$$\sigma_{x,y} \approx 17 \text{ microns}$$
$$\sigma_r \approx 13 \text{ microns}$$
$$\sigma_z \approx 480 \text{ microns}$$

Here x and y are the transverse dimensions, $r=\sqrt{x^2+y^2}$ and z is the dimension in the beam direction. The distributions of the residuals relative to the true position of the vertex of the decay in these coordinates are given in Figures 4a,b,c and d. To give a sense of the distances involved in B decay, we show in Figures 5a and b the Δz and Δr separations of the true decay vertices from the true primary vertex.

In the same way we have calculated the average residuals for primary vertices. Here as a model for 800 GeV/c pN interactions we have used 360 GeV/c bubble chamber events scaled up to 800 GeV/c. (The multiplicities are scaled by log S and the momentum of the secondaries by $\sqrt{S}$). We observe the Δx, Δy, Δr and Δz distributions shown in Figures 6a,b,c and d. The widths of these distributions are:

$$\sigma_{x,y} \approx 7 \text{ microns}$$
$$\sigma_r \approx 5 \text{ microns}$$
$$\sigma_z \approx 200 \text{ microns}$$

The residual distributions for the primary vertex are narrower than those of the secondary vertices because of the larger number of outgoing tracks.

Given these resolutions and the scale of the events, reasonable efficiencies for recognition of events with secondary vertices due to beauty decay can be achieved. A scatterplot of the Δz and Δr separation between the reconstructed primary and secondary decay vertices for typical beauty events (using only the decay muons for the secondary vertex) is shown in Figure 7a. The projections of this scatterplot are shown in Figures 7b and 7c. These projections can be compared to the true separations plotted in Figures 5a and b. In the Monte Carlo calculation used to obtain these distributions we have superimposed beauty decays of the type $B \longrightarrow \psi K\pi$ on the scaled bubble chamber events in order to get a realistic estimate of the reconstruction difficulties in

these complicated events. In this Monte Carlo smearing effects due to the misassignment of tracks from the other B decay to the primary vertex are included. A cut of Δz=1 mm and Δr=50 microns will retain 76% of the true beauty decays. Making a conservative estimate of composite efficiency (geometric acceptance is already taken into account) of the rest of the spectrometer (PWC's, drift chambers, etc.) of 80%, we expect to collect $\approx$ 60 % of the B—> ψ—>$\mu\mu$ decays given in Table VI.

In order to estimate the backgrounds to this signal, we have superimposed "ordinary" ψ production on the 800 GeV/c events and estimated the number of ψ's that will appear to form a false secondary vertex. Figures 8a, b and c gives the scatterplot and projections for reconstructed ψ's from the primary vertex corresponding to the scatterplot and projections for the true decays (Figures 7 a, b, c). The cuts of Δr> 50 microns and Δz>1mm which were chosen to select events containing true secondary vertices, reject 2.8×10^{-5} of all "ordinary" ψ events. In addition, if necessary, we can require that there be a third track that appears to come within 50 microns of the secondary vertex defined by the muons. This additional criterion reduces the remaining background from poorly reconstructed ψ's by an additional factor >10. Only a slight loss of signal is caused by this third track requirement. Thus we have an overall suppression of background $>2.8\times10^{-6}$.

Another experimental issue is the efficiency with which the muons, as identified and measured in the spectrometer proper, can be identified with a particular track as measured in the tracker. We have investigated the difficulties in matching the silicon detector tracks and the tracks as detected in the PWC's and drift chambers of the spectrometer. We have attempted to make matches both in angle and in intercept at various planes downstream of the third module of the silicon tracker. We conclude that there is little confusion in correlating the muon tracks with the appropriate tracks in the silicon tracker. We estimate <5% loss of dimuon events due to inability to correlate the muons with the correct tracker track.

In conclusion, after these cuts and efficiencies take their toll, we are left with **a few hundred to a few thousand** inclusive beauty—>ψ—>$\mu\mu$ decays (depending on the exact level of the cross section) with which to estimate cross sections for hadroproduction of beauty mesons. If the majority of these B's are beauty mesons B_u, B_d, or B_s, then there are several exclusive decay modes (see Table I) which have relatively simple topologies and which take place at the level of 10% of the B—>ψ+anything sample of events. It seems quite feasible to reconstruct the B mesons which decay into $\psi x^{\pm}$ or $\psi x^{+}y^{-}$. Some smaller portion of the events which have a single K^0 in the final state may be reconstructable. These K^0 events have the advantage that there is no two fold ambiguity in the identity of the strange particle which plagues the totally charged final states in the absence K-π identification. Those final states having more than one K^0 or a π^0 are much more difficult to reconstruct. We conclude that obtaining samples of several exclusive beauty decay modes containing a few 10's to a few 100's of totally reconstructed events seems definitely within the realm of feasibility.

Using the suppression of backgrounds obtained from the secondary vertex cuts and the requirement of a third track pointing at the secondary vertex, we estimate, using the number of ψ's from Table VII that are produced in our standard run, that we will have a background of a few 10's of fake events to our inclusive signal of a few hundred to a few thousand true B—>ψ—>$\mu\mu$ events. This background will be further reduced in our search for specific exclusive final states since we are trying in that case to reconstruct specific masses. Our mass resolution should be quite good, on the order of 20-30 MeV/c^2 for a final state such as $B^{-}_{\overline{u}}$—> $K^{-}\psi$, because the technique of fixing the ψ mass after the ψ is observed can be employed. This improvement in mass resolution should make negligible any remaining backgrounds to the exclusive decay signals.

C) pW —> $\overline{B}B$ + X : $\overline{B}^0B^0$ Mixing as detected by the semileptonic decays B^0 —>μ + ν + anything leading to same sign dimuons

The signal for this physics is same sign dimuons where each muon comes from a different neutral secondary vertex. The B^0 or $\overline{B^0}$ evolve into one another and then decay semileptonically thereby producing a same sign dimuon signal:

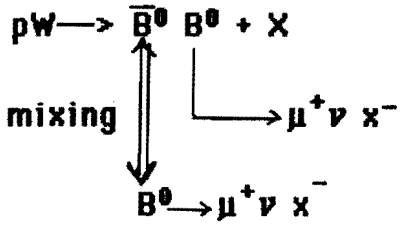

The semileptonic branching ratio for $B_{u,d}$—>μ+ν+hadrons is 12.4%. We assume that approximately this branching ratio is approximately the same for B_s. If we look for the simultaneous semileptonic decay of both the B's to detect $B^0\overline{B^0}$ mixing, we will observe 1.54×10^{-2} of all produced $B\overline{B}$ final states undergoing double semileptonic decay and producing opposite sign dimuons. If some of the B^0's evolve into their antiparticles then we will observe a same sign dimuon signal which is some fraction of this opposite sign dimuon signal. It is expected[20,21] that the majority of mixing occurs between $\overline{B^0}_s$ and B^0_s. The expected level of the mixing of the strange beauty meson is approximately[20,21] 20%. If B_d, B_u and B_s are produced equally copiously in the hadronization of the b quarks in pN interactions, then 4/9 of the possible $B\overline{B}$ final states will include one B^0_s meson that can evolve into a $\overline{B^0}_s$ meson and 1/9 of the final $B\overline{B}$ states will have two B^0_s mesons. Therefore,we would expect to see a like sign dimuon signal due to $B^0\overline{B^0}$ mixing which is 1.89×10^{-3} of all $B\overline{B}$ final states. The geometric acceptance for muons from double semileptonic decays of beauty has been estimated to be 25%. So we expect to see between 425 and 5200 same sign dimuons from mixing in comparison to the 3500 to 42400 opposite sign dimuon from the double semileptonic decays of B's produced in 800 GeV/c interactions depending on the cross section for beauty. For 925 GeV/c pW interactions we would expect to observe between 660 and 8100 same sign dimuons from mixing in comparison to 8200 to 40500 opposite sign dimuons.

The backgrounds to $B\bar{B}$ mixing come from several sources. The most serious background is produced by the sequential decay of one of the B's to a charmed daughter which decays semileptonically into a muon which has a different sign than would have been produced by the semileptonic decay of the parent B. This will produce a same sign dimuon background if the other B also decays semileptonically. There are several decay chains which result in this sort of "daughter charmed particle" same sign background to $B\bar{B}$ mixing. Under the assumptions 1) that B_u, B_d and B_s are made equally frequently and 2) that the various reported branching ratios (the ratios that are used are either preliminary results from the CLEO experiment[22] or reported ratios from the particle data tables[23]) for decays of unseparated mixtures of $B_d^0, \bar{B}_d^0, B_u^+, B_u^-$ can be used both for the individual beauty mesons and for B^0_s mesons, we can evaluated the backgrounds due to the decay sequences listed below:

1. Charged B plus neutral B production followed by decay of $B^{\pm} \rightarrow D^{\bar{0}, 0}$:

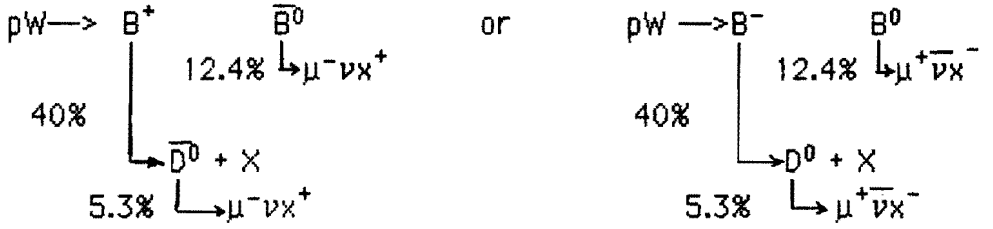

Thus, 2.6×10^{-3} of the $B^+\bar{B}^0 + B^-B^0$ production (4/9 of all $b\bar{b}$ pairs) decays via these chains to produce a background of 260 to 3200 same sign dimuons in a canonical 800 GeV/c run.

2. Charged B plus neutral B production followed by decay of $B^{\pm} \rightarrow D^{\pm}$:

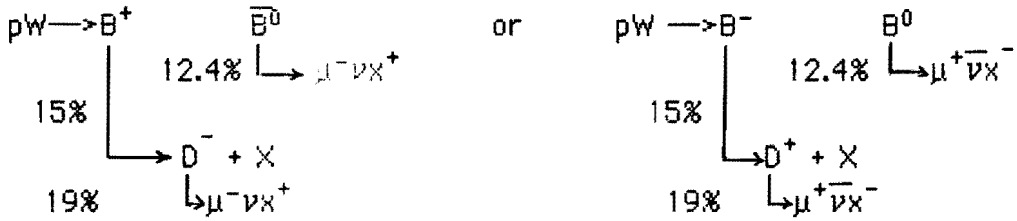

An additional 3.5×10^{-3} of the $B^+\overline{B^0}$ + B^-B^0 production (4/9 of all $b\overline{b}$ production) will decay via charged D's into a same sign dimuon background of 350 to 4300 events in the 800 GeV/c run.

3. Charged B plus neutral B production followed by decay of $B^{0,\overline{0}} \rightarrow \overline{D^0}, D^0$

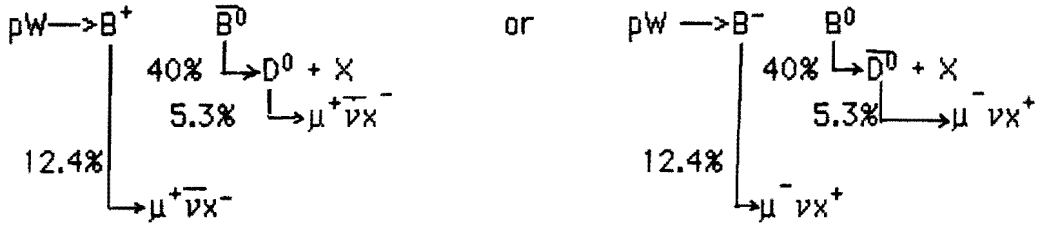

This decay chain is responsible for an additional 2.6×10^{-3} of the $B^+\overline{B^0}$ $+B^-B^0$ production decaying to a same sign background of 260 to 3200 events

4. Charged B + neutral B production followed by decay of $B^{0,\overline{0}} \rightarrow D^-, D^+$

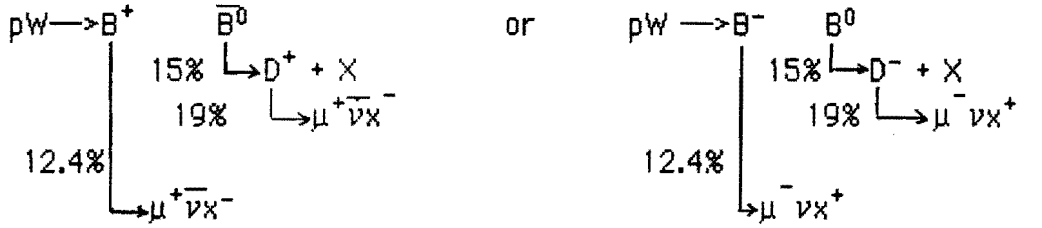

Finally, this decay chain is responsible for an additional 3.5×10^{-3} of the $B^+\overline{B^0}$ $+B^-B^0$ production decaying to a background of 350 to 4300 events.

5. Neutral B production followed by decay of $B^{0,\overline{0}} \rightarrow \overline{D^0}, D^0$

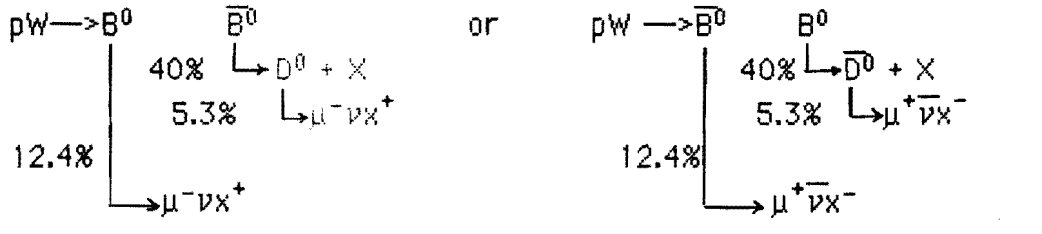

This decay sequence results in 2.6% of the $B^0\overline{B}^0$ final states (4/9 of the total $b\overline{b}$ production) decaying into a same sign background which contains 260 to 3200 events for the 800 GeV/c run.

6. Neutral B production followed by decay of $B^{0,\overline{0}} \rightarrow D^-, D^+$

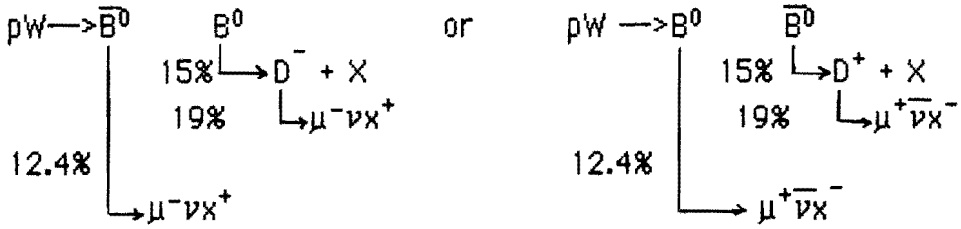

3.5×10^{-3} of the $B^0\overline{B}^0$ production (4/9 of the entire $b\overline{b}$ production) decays via this chain to a same sign dimuon background of 350 to 4300 events.

7. Charged B production followed by decay of $B^{\pm} \rightarrow D^{\pm}$

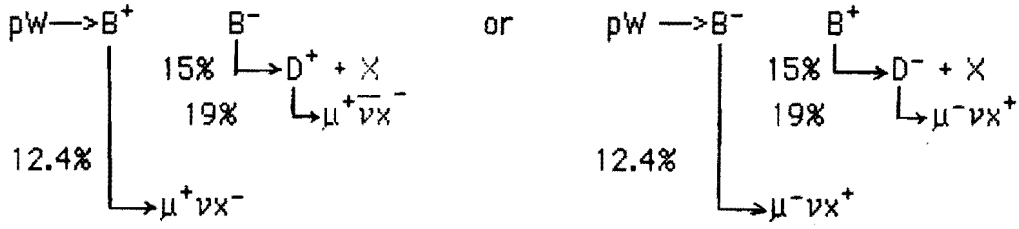

3.5×10^{-3} of the B^+B^- final states (1/9 of all $b\overline{b}$ final states) decay via this sequence to a same sign muon background of 90 to 1070 events.

8. Charged B production followed by decay of $B^{\pm} \rightarrow \overline{D}^0, D^0$

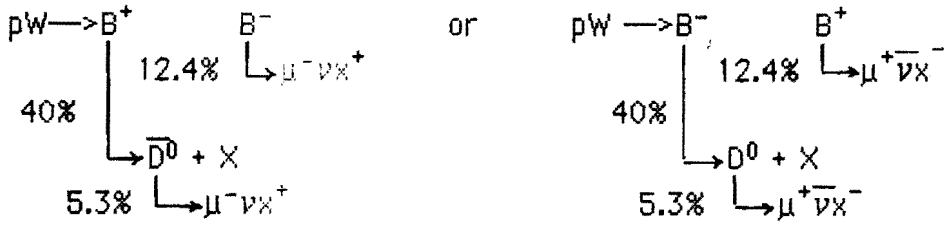

2.6×10^3 of the B^+B^- final states (1/9 of all $b\bar{b}$ final states) decay via this sequence producing a same sign muon background of 70 to 800 events.

Thus, the total same sign background from the sum of these sequences, in the absence of any cuts to suppress them, would be 2000 to 24000 events to be compared to a $B^0\bar{B}^0$ mixing signal of 660 to 8100 events in an 800 GeV/c run. So our signal to background is 1/3 from the charmed daughter decay sequences without cuts.

The second same sign background to $B\bar{B}$ mixing is production of $D^0\bar{D}^0$ followed by mixing and the subsequent semileptonic decay of the charmed particles. In this case the semileptonic decay branching ratio is 5.3% for the D^0 and the mixing between D^0 and $\bar{D}^0$ is small (<.006 experimentally[24] and estimated theoretically[20,21] to be between 10^{-4} and 10^{-7}). Taking the largest theoretical rate and assuming that we have the same acceptance (25%) for the background dimuons as for the mixing dimuons, we would expect to see a same sign background of 60 to 770 like sign dimuons from $D^0\bar{D}^0$ mixing even if the charm cross section is 1000 times as large as the beauty cross section at 800 GeV/c.

The third background to $B\bar{B}$ mixing that we have considered is produced when one of the B's decays semileptonically and the other B decays nonleptonically. Then if one of the pion decay products of the second B decay itself decays into $\mu\nu$, a same sign background can be produced. Approximately 1% of the beauty decays produces a muon via $\pi\rightarrow\mu\nu$ so that we would expect 30 to 340 same sign background events from this source.

We have examined the possibility that we can further suppress these backgrounds (especially the "daughter" background) by cutting to the high mass μ pairs which should be relatively rich in the muons from beauty decay. Using the $B\bar{B}$ production model of appendix B, we have generated the like sign dimuon mass spectrum for the $B\bar{B}$ mixing signal and for each of the three backgrounds mentioned above: $B\rightarrow C\rightarrow\mu$, $C\bar{C}$ mixing and $B\rightarrow\pi\rightarrow\mu$. These four dimuon mass spectra are shown in

Figure 9. These spectra have arbitrary normalizations with respect to each other but the shapes of the spectra can be compared. For masses above 3 GeV/c^2 42% of the true mixing signal is retained while only 19%, 19% and 25% respectively of the three backgrounds survive. Therefore, improvements of a factor of two are realized in the ratio of signal to background in the high mass region.

A second technique for suppression of these backgrounds to $B\bar{B}$ mixing is the reconstruction of the "visible" mass of the secondary vertex. We show in Figures 10a and b the visible mass of the secondary vertex from

$$B^0 \rightarrow K\ \pi\ \pi\ \mu\ \nu$$

in comparison to the visible mass from

$$D^0 \rightarrow K\ \pi\ \pi\ \mu\ \nu$$

if the correct assignment of the right tracks to a given secondary vertex can be accomplished. These figures show that for a perfect assignment of tracks, 98% of the beauty secondary decay vertices with this topology have masses above 2.0 GeV/c^2 and can be cleanly separated from the D^0 decays with the same topology. In addition, if a 100% correct assignment of tracks to specific vertices could be accomplished, then one could require the neutrality of each pair of secondary vertices with a muon track before the event was added to the mixing sample of events. This would eliminate all but the daughter decay sequences 5 and 6 exclusive of the irreducible backgrounds due to charged D's decaying too near to their parent B^0 decays to be resolved or of neutral D's decaying too far from the parent $B^{\pm}$ decay to be associated with that parent. Figures 11a and b show the longitudinal and transverse separation of the daughter D decay vertices from their parent vertices.

However, a completely correct assignment of all tracks associated with a particular secondary vertex to that vertex is very difficult since mistakes can be made either by adding tracks or losing them. This is especially true for the mixing event topology [9] in distinction to the ψ

topology) in which there are only pairs of muons from different vertices to flag the events and to begin the process of reconstruction of a secondary vertex. If one can begin by developing a technique for finding secondary vertices in such events then the association of the tracks with these vertices can proceed given the track resolutions possible with silicon trackers. We show in Figures 12 a, b, c and d the distance from the true decay vertex that the reconstructed primary and secondary tracks pass. As a first attempt at solving this problem, we have partially investigated one possible technique for defining secondary vertices and assigning tracks to them. The steps in this iterative procedure are as follows:

1. Form a first order primary vertex from fits of all tracks in the event excluding the muon tracks. The resolution of the primary vertex for $B\bar{B}$ events is $\approx$ 21 microns due to the broadening by the tracks from the secondary vertices.

2. Choose tracks to be associated with the primary vertex by excluding those a distances greater than 50 microns from the first order vertex.

3. Form the second order primary vertex by fitting this track sample. The second order vertex resolution now is 7.3 microns in agreement with the true resolution for primary vertices.

4. Demand that the muon track be separated by 50 microns in the transverse dimension at the target midplane from this second order vertex just formed. As shown in Figure 13a and b, this cut loses 50% of the muons from B decay but eliminates 98% of the tracks from the primary vertex from candidacy for secondary tracks.

5. Demand that any track that is to be associated with the secondary muon pass within a distance $\sqrt{(\Delta x^2+\Delta y^2+\Delta z^2)}$ =50 microns of the muon at the distance of closest approach.

Using these criteria we have selected decay muons and associate

secondary tracks with those muons for samples of events containing $B\bar{B}$ decays and $D\bar{D}$ decays into $K\pi\pi\mu\nu$ to test the technique. For the sample of chosen tracks which appear to be associated with the decay muons we have formed the visible mass. Figures 15a and b show this mass for these samples. We see that the "B" masses go below 2 GeV/c^2 because of the loss of tracks and far above 5.3 GeV/c^2 because of the inclusion of tracks not belonging to the secondary vertex. Obviously more iterations would help to eliminate these losses and inclusions as the fits of the vertex improves. However, even at this relative simple stage with the relatively naive algorithm for determining a vertex, the visible mass is still a useful tool. A cut at 3 GeV/c^2 will eliminate 40% of the D mesons while keeping 88% of the B decays.

Therefore, use of this crude version of visible mass should make another factor of 2 in mixing signal to background ratio. Taken in conjunction with the selection of high mass events, we should achieve signal to background ratios greater than 1 for limited samples ($\approx$10%) of the same sign events. It should, however, be possible to find better procedures and algorithms to define the secondary vertices and associate the proper tracks with them.

D) p W $\longrightarrow \chi_c$ + anything : $\chi_c \longrightarrow \gamma\psi$: $\psi \longrightarrow \mu\mu$

The study of the production of χ_c states that we are presently engaged in will be continued at higher energies with the extracted proton beam. The measurement of hadroproduction of χ's allows us to study gluon fusion and the structure function of the gluon especially in the case of pN interactions. We refer the reader to the E-705 proposal[1] for a more extensive discussion of this topic. We will have data with protons at 300 GeV/c so energy dependent effects can be studied. We list in Table VII our expectations for data at 800 and 925 GeV/c assuming that 30.5% of the observed ψ's are produced from the decays of χ's via the $\gamma\psi$ decay mode just as is the case at lower energies. The A dependence used to scale these cross sections to the W target is $A^{0.32}$.

Table VII

Energy	$\sigma(pN \rightarrow \psi)$	$Acceptance_{\chi}$	$N_{\psi \rightarrow \mu\mu}$	$N_{\chi \rightarrow \psi\gamma \rightarrow \gamma\mu\mu}$
800 GeV/c	600 nb	0.132	$\approx 1.4\times10^{6}$	4.2×10^{5}
925 GeV/c	800 nb	0.110	$\approx 1.5\times10^{6}$	4.6×10^{5}

E) p W —> χ_b + anything : χ_b—>$\gamma\Upsilon$: Υ —>$\mu\mu$

The same sequence of decays that was used to detect χ_c can be used to detect χ_b states of the bound $B\overline{B}$ system. Using the model for $\Upsilon(9460)$ production in pp interactions of reference 15 which has been fit to the experimental data of reference 25 and 26, we predict $\sigma(pp \rightarrow \Upsilon + X) \approx 6\times10^{-34}$ cm^2 at 800 GeV/c and 8×10^{-34} cm^2 at 925 GeV/c. These cross sections yield approximately 22500 and 30000 Υ's at 800 and 925 GeV/c for our canonical run. The branching ratio[23], $BR(\Upsilon \rightarrow \mu\mu) = 0.0291$ so the total number of $\Upsilon \rightarrow \mu\mu$ observed in our run will be 650 or 900 at 800 or 925 GeV/c respectively. While the number of χ_b which cascade through the decay chain $\chi_b \rightarrow \gamma\Upsilon \rightarrow \gamma\mu\mu$ is unknown, an inspection of the χ_b branching ratios into $\gamma\Upsilon$ makes it tempting to surmise that 1/3 of the Υ production occurs through this sequence (as is the case for $\chi_c \rightarrow \gamma\psi$). If this is the case we can expect 200 or 300 $\chi_b \rightarrow \gamma\Upsilon \rightarrow \gamma\mu\mu$ before acceptance cuts and reconstruction efficiencies are imposed. Making reasonable estimates for these factors, we should be left with a several 10's of events at these energies. This would be sufficient for a first observation of the hadroproduction of χ_b.

VII. Conclusions

The study of the heavy quark states produced using the highest energy proton beam available with the E-705 spectrometer offers an exciting opportunity. This spectrometer is particularly well suited because of the long history of studying dimuon final states to look for beauty associated with dimuons. The addition of a silicon tracker is

necessary in order to detect the secondary decay vertices and the presence of a ψ produced in such a secondary vertex will ensure that beauty decay is being observed. The sophistication of our dimuon trigger and trigger processor and the development of a data acquisition system capable of handling large data flows makes this experiment uniquely able to run at a rate (in an open geometry) necessary to make accessible the beauty cross sections.

Appendix A

Upgrade of the High Intensity Laboratory Secondary Beam Transport

This appendix describes an upgrade of the secondary beam transport in the P-West High Intensity Laboratory that will allow, as a first objective, transport of the primary proton beam (800->925 GeV/c) to the E-705 spectrometer. In addition, this modified beam line will allow the transport and focussing of higher energy pions on the E-705 target than is possible with the present beam line. The expected yield and spot sizes of the modified beam are given for 300 GeV/c π^- (in comparison with the present 300 GeV/c π^- beam), 600 GeV/c π^- and 800->925 GeV/c protons. The modified 300 GeV/c $\pi/\overline{p}$ tune is preferred over the present tune of the beam line because of higher yield but may require more power supplies than are currently used. None of the three new configurations, 300 GeV/c $\pi^-/\overline{p}$ tune, the 600 GeV/c π^- transport, or the 800/925 GeV/c primary proton transport require more quadrupoles but the higher energy beams will require more bending magnets. We have determined that our prime objective in this upgrade is the transport of the primary protons to the experiment target and have configured the transport to do that with no loss of acceptance at 300 GeV/c for $\pi/\overline{p}$ and with reasonable acceptance for π^- at higher energies.

Table A1 gives the present 300 GeV/c beam configuration and tune. The first set of names of the beam elements anticipates the beam line upgrade that is being proposed. The second set of names given to each beam element is their present designation according to the standard laboratory naming system.

Table A1
Present 300 GeV/c $\pi^-/\bar{p}$ Beam

Beam Section	Beam Elements				Present 300 GeV/c $\pi^-/\bar{p}$ Beam Tune		
	Name		Type	Z Location*	Field (kG,kG/in)	Current (amp)	Power (kW)
Target	B1	PW6W2	B2	1.96'	15.5	4100	47.7
Box Bend							
Flux	Q1-1	PW6Q1-1	4Q120	47.40'	6.09	1500	32.5
Collection	Q1-2	PW6Q2-1	4Q120	69.31'	-5.56	1250	22.6
Triplet	Q1-3	PW6Q2-2	4Q120	80.77'	-5.56	1250	22.6
	Q1-4	PW6Q1-2	4Q120	95.77'	6.09	1500	32.5
Momentum	B2-3	PW6W3-1	6-3-120	146.32'	17.7	1220	29.3
Selection	B2-4	PW6W3-2	6-3-120	157.82'	17.7	1220	29.3
Bend=10.94 mr							
Momentum Slit -		-	-	230.95'	-	-	-
FODO	Q2-1	PW6Q4-1	4Q120	295.93'	5.21	1080	16.9
Channel	Q2-2	PW6Q4-2	4Q120	352.72'	-5.21	1080	16.9
5.79 mr-->	B3-2	PW7W1-1	6-3-120	375.39'	17.1**	1180	27.4
	Q2-3	PW6Q4-3	4Q120	433.63'	5.21	1080	16.9
12.25 mr->	B4-2	PW7W2-1	Mod B1	458.27'	18.1**	1090	41.5
	B4-3	PW7W2-2	Mod B1	469.27'	18.1**	1090	41.5
	Q2-4	PW6Q4-4	4Q120	490.36'	-5.21	1080	16.9
5.79 mr-->	B3-5	PW7W1-2	6-3-120	512.36'	17.1**	1180	27.4
Targeting	Q3-1	PW7Q1	4Q120	571.97'	3.99	740	7.9
Triplet	Q3-2	PW7Q2-1	4Q120	608.01'	-3.61	696	7.0
	Q3-3	PW7Q2-1	4Q120	619.68'	-3.61	696	7.0
	Q3-4	PW7Q3	4Q120	654.26'	4.47	836	10.1
E-705 Target -		-	-	878.89'	-	-	-

* Approximate Z locations measured in feet from the primary production target to the upstream end of the magnet in question.

**The apparent inconsistency between three bend due to the settings of the magnets PW7W1 and PW7W2 in the present 300 GeV/c tune and the actual 4.84,14.15 and 4.84 mrad geometric bends that are built into the P-West secondary beam is due to the lack of adequate strength in

the two modified B2's to make the 14.15 mrad bend in the middle of the FODO channel. The total bend in the FODO channel is accomplished by 'sharing' the bend, driving PW7W1-1 and PW7W1-2 harder to compensate for the underbending of PW7W2-1,2. This produces an undesirable skewed trajectory through the transport system for the $\pi^-/\bar{p}$ flux and loses horizonal aperture for the $\bar{p}/\pi^-$ beam.

The values of the fields are calculated from the transfer functions published in reference 27. A negative field for a quadrupole indicates vertical focussing of a beam according to the convention of TURTLE ray tracing program[28]. The currents in the magnets are those documented as of August 20,1985 (3:13 PM) during the last E-705 run. A RMS factor of 0.63 (suggested by A. Visser) based on the ramping of the magnets for the 23 second spill has been used to calculate the power consumption of the magnets. The cable losses have been ignored since they are less than 1-2% (A. Visser-private communication). The total power consumption of the beam line elements listed in Table A1 is 455 kW or 700 kVA to be compared with the total installed substation capacity of 6000 kVA in the High Intensity Laboratory. The substation kVA loading will be higher when calculated for the actual power supply configuration needed and when all other loads (pumps, small magnets, analysis magnets, etc) are included in the total.

The beam tune given above is that used for either the $\bar{\Lambda}^0 \rightarrow \bar{p}$ beam or the ordinary high intensity secondary π^- beam as established during the 1985 run of E-705. The difference between the tertiary $\bar{p}$ beam and the secondary π beam is the targeting of the incident primary proton beam and the setting of the P-West target box B-2 sweeping magnet. The high setting for the target box magnet shown in Table A1 is the setting for the $\bar{\Lambda}^0$ beam. The yield of the π^- according to the Stefanski-White production model in an angular range about zero degrees of $\theta_x=\pm 3.0$ mrad, $\theta_y=\pm 3.0$ mrad and within a momentum bite of $\Delta p/p=\pm 50\%$ about 300 GeV/c is .0414 π^- per 800 GeV/c primary proton. For the beam tune shown in Table A1 the ray tracing program TURTLE predicts that .0274 of those pions will survive the beam transport and be focussed on the E-705 target. This leads to an overall yield of

1.13×10^{-3} 300 GeV/c π^- per 800 GeV/c proton. One of the criteria that we have used for our proposed upgrade is that we maintain this yield at 300 GeV/c while adding the capability of transport of the 800 (or 925) GeV/c primary protons to the E-705 target. The predicted spot sizes at the E-705 target are $\sigma_x\approx1.7$ cm and $\sigma_y\approx1.6$ cm in reasonable agreement with the spot sizes observed during the 1985 run of E-705.

Table A2 gives the configuration of the proposed new transport with the improved new 300 GeV/c tune. As can be seen by comparison of Table A1 with Table A2, no new quadrupoles have been added and the positions of the already installed quadrupoles have not changed. The only additions or modifications to the beam transport are the eight new bending magnets (shown in bold face type) and the rearrangement of the two modified B2 bending magnets to allow the insertion of enough bending power to handle 800(925) GeV/c primary protons. While the 300 GeV/c tune of the present beam will work with this modified beam we have improved the tune of the quadrupole system in the process of developing the new transport. The new tune gives yields 2.24×10^{-3} 300 GeV/c π^- per 800 GeV/c proton, approximately twice that of the present tune. The spot sizes ($\sigma_x\approx1.4$ cm and $\sigma_y\approx1.6$ cm) are slightly better than those of the tune of Table A1. The total power consumed is 402 kW or 618 kVA, slightly less than that of the present tune due to the additional bending power available.

Table A2
Proposed 800(925) GeV/c Transport
300 GeV/c $\pi^-/\bar{p}$ Tune

Beam Section	Beam Elements				New 300 GeV/c $\pi^-/\bar{p}$ Beam Tune		
	Name	Type	Z Location	Field (kG,kG/in)	Current (amp)	Power (kW)
Target Box Bend	B1	PW6W2	B2	1.96'	15.5	4100	47.7

Flux	Q1-1	PW6Q1-1	4Q120	47.40'	6.09	1500	32.5
Collection	Q1-2	PW6Q2-1	4Q120	69.31'	-6.09	1500	32.5
Triplet	Q1-3	PW6Q2-2	4Q120	80.77'	-6.09	1500	32.5
	Q1-4	PW6Q1-2	4Q120	95.77'	6.09	1500	32.5
Momentum	**B2-1**	-	**6-3-120**	123.32'	5.42	310	1.9
Selection	**B2-2**	-	**6-3-120**	134.82'	5.42	310	1.9
Bend	B2-3	PW6W3-1	6-3-120	146.32'	5.42	310	1.9
10.94 mr	B2-4	PW6W3-2	6-3-120	157.82'	5.42	310	1.9
	B2-5	-	**6-3-120**	169.32'	5.42	310	1.9
	B2-6	-	**6-3-120**	180.82'	5.42	310	1.9
Momentum Slit -		-	-	230.95'	-	-	-
FODO	Q2-1	PW6Q4-1	4Q120	295.93'	6.09	1500	32.5
Channel	Q2-2	PW6Q4-2	4Q120	352.72'	-6.09	1500	32.5
	B3-1	-	**6-3-120**	364.39'	4.77	300	2.8
4.84 mr-->	B3-2	PW7W1-1	6-3-120	375.39'	4.77	300	2.8
	B3-3	-	**6-3-120**	386.39'	4.77	300	2.8
	B4-1	PW7W2-1	Mod B1	422.13'	6.97	420	6.2
	Q2-3	PW6Q4-3	4Q120	433.63'	6.09	1500	32.5
14.15 mr->	**B4-2**	-	**B2**	448.27'	6.97	1700	8.2
	B4-3	-	**B2**	469.27'	6.97	1700	8.2
	Q2-4	PW6Q4-4	4Q120	490.36'	-6.09	1500	32.5
	B4-4	PW7W2-1	Mod B1	502.36'	6.97	420	6.2
	B3-4	-	**6-3-120**	512.36'	4.77	300	2.8
4.84 mr-->	B3-5	PW7W1-2	6-3-120	523.36'	4.77	300	2.8
	B3-6	-	**6-3-120**	534.36'	4.77	300	2.8
Targeting	Q3-1	PW7Q1	4Q120	571.97'	4.87	950	13.0
Triplet	Q3-2	PW7Q2-1	4Q120	608.01'	-3.25	625	5.6
	Q3-3	PW7Q2-1	4Q120	619.68'	-3.25	625	5.6
	Q3-4	PW7Q3	4Q120	654.26'	4.87	925	13.0
E-705 Target -		-	-	878.89'	-	-	-

In Table A3 below we show the 600 GeV/c tune of the modified beam transport. With this tune we expect a yield of 6.57×10^{-5} 600 GeV/c π^- per 800 GeV/c primary proton. The spot sizes at the E-705 experimental target are somewhat worse ($\sigma_x\approx3.5$ cm and $\sigma_y\approx1.5$ cm)

due to chromatic aberrations since the emphasis at this higher energy was placed on collection of flux rather than minimizing spot size. The total power required to transport and focus the 600 GeV/c π^- beam is 466 kW or 716 kVA quite comparable to present power usage of the present 300 GeV/c transport.

Table A3
Proposed 800(925) GeV/c Transport
600 GeV/c π^- Tune

Beam Section	Beam Elements				600 GeV/c π^- Beam Tune		
	Name		Type	Z Location	Field (kG,kG/in)	Current (amp)	Power (kW)
Target	B1	PW6W2	B2	1.96'	13.2	3300	30.9
Box Bend							
Flux	Q1-1	PW6Q1-1	4Q120	47.40'	4.09	750	8.1
Collection	Q1-2	PW6Q2-1	4Q120	69.31'	-6.09	1500	32.5
Triplet	Q1-3	PW6Q2-2	4Q120	80.77'	-6.09	1500	32.5
	Q1-4	PW6Q1-2	4Q120	95.77'	4.09	750	8.1
Momentum	**B2-1**	-	**6-3-120**	123.32'	10.8	650	8.3
Selection	**B2-2**	-	**6-3-120**	134.82'	10.8	650	8.3
Bend	B2-3	PW6W3-1	6-3-120	146.32'	10.8	650	8.3
10.94 mr	B2-4	PW6W3-2	6-3-120	157.82'	10.8	650	8.3
	B2-5	-	**6-3-120**	169.32'	10.8	650	8.3
	B2-6	-	**6-3-120**	180.82'	10.8	650	8.3
Momentum Slit	-	-	-	230.95'	-	-	-
FODO	Q2-1	PW6Q4-1	4Q120	295.93'	6.09	1500	32.5
Channel	Q2-2	PW6Q4-2	4Q120	352.72'	-6.09	1500	32.5
	B3-1	-	**6-3-120**	364.39'	9.50	575	6.5
4.84 mr-->	B3-2	PW7W1-1	6-3-120	375.39'	9.50	575	6.5
	B3-3	-	**6-3-120**	386.39'	9.50	575	6.5
	B4-1	PW7W2-1	Mod B1	422.13'	13.9	837	24.5
	Q2-3	PW6Q4-3	4Q120	433.63'	4.09	750	8.1
14.15 mr->	**B4-2**	-	**B2**	448.27'	13.9	3450	34.3

	B4-3	-	**B2**	469.27'	13.9	3450	34.3
	Q2-4	PW6Q4-4	4Q120	490.36'	4.09	750	8.1
	B4-4	PW7W2-1	Mod B1	502.36'	13.9	837	24.5
	B3-4	-	**6-3-120**	512.36'	9.50	575	6.5
4.84 mr-->	B3-5	PW7W1-2	6-3-120	523.36'	9.50	575	6.5
	B3-6	-	**6-3-120**	534.36'	9.50	575	6.5
Targeting	Q3-1	PW7Q1	4Q120	571.97'	4.09	750	8.1
Triplet	Q3-2	PW7Q2-1	4Q120	608.01'	-4.80	936	12.7
	Q3-3	PW7Q2-1	4Q120	619.68'	-4.80	936	12.7
	Q3-4	PW7Q3	4Q120	654.26'	6.09	1500	32.5
E-705 Target	-	-	-	878.89'	-	-	-

Finally in Table A4 we give the tune of the beam for transport and focussing of 800(925) GeV/c primary protons. As can be noted all quadrupoles in the transport except for the targeting triplet have been turned off. The protons can be focussed to a 1.8 mm × 1.8 mm spot at the E-705 target. The total power consumption for the 800(925) GeV/c beam is 406(630) kW or 625(970) kVA.

Table A4
Proposed 800(925) GeV/c Transport*
800(925) GeV/c Primary Proton Tune

Beam Section	Beam Element		800(925) GeV/c Proton Beam Tune		
	Name	Type	Field (kG,kG/in)	Current (amp)	Power (kW)
Target**	B1	B2	-	-	-
Box Bend					
Flux	Q1-1	4Q120	-	-	-
Collection	Q1-2	4Q120	-	-	-
Triplet	Q1-3	4Q120	-	-	-
	Q1-4	4Q120	-	-	-
Momentum	**B2-1**	**6-3-120**	14.4(16.6)	860(1070)	14.5(22.5)
Selection	**B2-2**	**6-3-120**	14.4(16.6)	860(1070)	14.5(22.5)
Bend	B2-3	6-3-120	14.4(16.6)	860(1070)	14.5(22.5)

10.94 mr-->	B2-4	6-3-120	14.4(16.6)	860(1070)	14.5(22.5)
	B2-5	**6-3-120**	14.4(16.6)	860(1070)	14.5(22.5)
	B2-6	**6-3-120**	14.4(16.6)	860(1070)	14.5(22.5)
Momentum Slit -		-	-	-	-
FODO***	Q2-1	4Q120	-	-	-
Channel	Q2-2	4Q120	-	-	-
	B3-1	**6-3-120**	13.3(18.2)	775(1370)	11.8(36.9)
5.05 mr-->	B3-2	6-3-120	13.3(18.2)	775(1370)	11.8(36.9)
(5.98)	**B3-3**	**6-3-120**	13.3(18.2)	775(1370)	11.8(36.9)
	B4-1	Mod B1^{+}	18.1(18.1)	1090(1090)	41.5(41.5)
	Q2-3	4Q120	-	-	-
13.72 mr->	**B4-2**	**B2**	18.0(18.0)	4700(4700)	62.8(62.8)
(11.88)	**B4-3**	**B2**	18.0(18.0)	4700(4700)	62.8(62.8)
	Q2-4	4Q120	-	-	-
	B4-4	Mod B1^{+}	18.1(18.1)	1090(1090)	41.5(41.5)
	B3-4	**6-3-120**	13.3(18.2)	775(1370)	11.8(36.9)
5.05 mr-->	B3-5	6-3-120	13.3(18.2)	775(1370)	11.8(36.9)
(5.98)	**B3-6**	**6-3-120**	13.3(18.2)	775(1370)	11.8(36.9)
Targeting	Q3-1	4Q120	4.88(5.64)	950(1275)	13.0(23.5)
Triplet	Q3-2	4Q120	-3.60(4.16)	696(800)	7.0(9.2)
	Q3-3	4Q120	-3.60(4.16)	696(800)	7.0(9.2)
	Q3-4	4Q120	4.88(5.64)	950(1275)	13.0(23.5)
E-705 Target -		-	-	-	-

* Quantities in parenthesis refer to the 925 GeV/c values of the parameters in question.

** The target box B2 is turned off in this tune anticipating that a zero degree trajectory can be achieved through the target box by a suitable combination of the pretarget bending magnets. If this is not the case then the target box magnet must be used to help deflect the 800(925) GeV/c proton beam into the proper trajectory.

***As is the case in the present 300 GeV/c π^- beam the central bend of 14.15 mrad cannot be made by the installed magnets. However in the case of the 800(925) GeV/c primary proton beam with its tiny size and momentum bite we can safely share the bend as long as we achieve a total bend of 23.83 mrad. The net displacement of the few mm proton beam at the central 14.15 mrad bend is only .2(.92) inches which presents no problem because of the 4 inch horizonal

aperture available in the main ring B2's positioned at that point.

+ The 18.1 kG is probably not attainable with the modified B1 magnets and therefore the small 5 foot trim magnets that are used in the current 300 GeV/c beam to augment the modified B1 will have to continue to be used in the same role.

In conclusion, the new transport system which will give the performance discussed above will require the new bending magnets listed below plus any attendant power supplies which will be required to operate them in the modes suggested in Tables II,III and IV:

1. 6-3-120 Bending Magnets (8)
2. Main Ring B-2-240 Bending Magnets (2)

The upgrade will be totally conventional and will fit within the existing transport with only minor rearrangements of positions. The total power consumption of the beam as given in the three tables does not seem prohibitive relative to the power consumption of the 300 GeV/c $\Lambda^0 \rightarrow \bar{p}$ beam already in operation. We point out that our choice of bending magnets to implement the modified beam is not the only way to achieve the requisite bends at 800(925) GeV/c but any other solution must be checked to see that it maintains the acceptance of the secondary beam.

Appendix B

Model for Production and Decay of Beauty Mesons

A simple model has been used to simulate the associated production of $B\bar{B}$ meson in pW interactions for the purposes of calculating the efficiencies and acceptances of this proposal. The individual B mesons are generated essentially uncorrelated with the second B meson with the following x_F and p_t distributions:

$$\frac{d\sigma}{dp_t} \propto \frac{1}{p_t^2 + M_b^2} \qquad \text{where } M_b = 5.3 \text{ GeV/c}^2$$

$$\frac{d\sigma}{dx_F} \propto e^{-x_F/9.8}$$

These distributions have been suggested[28] as appropriate for a rough description of B production. The x_F, p_t and p_z distributions that result from these functions are shown in Figures 12a, b and c with the average $p_t \approx 8.7$ GeV/c and the average $p_z \approx 237$ GeV/c for B's from 800 GeV/c pN interactions. The various decays of the B's that have been investigated in the proposal have been assumed to be isotropic in the rest frame of the B. For example, we shown the predicted p_t and p_z distributions of the ψ from $B \rightarrow \psi K\pi$ in Figures 13a and b. The K and π from this decay are quite stiff with $\langle p_K \rangle \approx 48$ GeV/c and $\langle p_\pi \rangle \approx 38$ GeV/c. Finally, for all calculations we have assumed a lifetime of all of the B meson varieties (B_u,B_d,B_s) of 0.6×10^{-12} seconds.

References

1. M. Binkley et al, Fermilab Proposal E-705, (October 1981).

2. H. Areti et al, A Fast Trigger Processor for Dilepton Triggers, Nuclear Instruments and Methods, A212 , 135 (1983).

3. E. Anassontzis et al, A Large Aperture Spectrometer to Study Dimuons, Nuclear Instruments and Methods, A242 , 215(1985).

4. E. Anassontzis et al, Continuum Dimuon Production in $\bar{p}W$ Collisions at 125 GeV/c, Phys. Rev. Letters, 54 , 2572 (1985).

5. P. Karchin, Performance of a Silicon Microstrip Vertex Detector in a Charm Photoproduction Experiment: Fermilab E691, to be published in the Proceedings of the UCLA Workshop on SSC Physics, (Jan, 1986).

6. B. Cox, The High Intensity Laboratory, Fermilab Report 79/1, 0090.1, (1979).

7. ARGUS Collaboration, DESY 85-070, Also see R. Davis, Proceedings of the American Physical Society, Eugene, Oregon (Aug,1985) to be published. Also R. Orr, Proceedings of the Lake Louise Winter Institute, Alberta, Canada (1986).

8. CLEO Collaboration, Also see R. Davis, Proceedings of the American Physical Society, Eugene, Oregon (Aug,1985) to be published. Also see M.S. Alam, Proceedings of the Lake Louise Winter Institute, Alberta, Canada (1986).

9. J.P. Albanese et al, WA75 Collaboration, CERN/EP 85-76.

10. E.H. Thorndike, to be published in the Proceedings of the 1985 International Symposium on Leptons and Photon Interactions, Kyoto, (Aug,1985).

11. C. Caso, New Flavor Production in Hadronic Interactions, CERN/EP-180, (Nov,1985).

12. J.D. Bjorken, private communication, (July, 1985).

13. M.G.D. Gilchriese, private communication, CBX 86-17.

14. C. Quigg, Memo to Taiji Yamanouchi, (July 16, 1985).

15. Y. Afek, C. Leroy and B. Margolis, Physical Review D, Vol 22, 1, 86(1982).

16. B.L. Combridge, Nuclear Physics B151, 429(1979).

17. J. Owens, private communication.

18. F. Halzen, 'Production of Heavy Quarks', Proceedings of the 21st International Conference on High Energy Physics, Paris, C3-381(1982).

19. D. Treille, 'Hard Scattering of Hadrons and Photons', Proceedings of the Int. Conference on High Energy Physics, Bari, Sicily (1985).

20. A. Ali and C. Jarlskog, Physics Letters 144B, 266(1984).

21. A. Ali, Heavy Flavor Production and Weak Mixings, Proceedings of the International Symposium on the Physics of $\overline{p}p$ Collisions, Tsukuba, 456(March,1985).

22. M.G.D. Gilchriese, private communication.

23. C.G. Wohl et al, Reviews of Particle Properties, Reviews of Modern Physics, 56, S190 (1984).

24. W.C. Louis et. al., Phys. Rev. Lettrs., 56, 1027(1986).

25. K. Ueno et al, Phys. Rev. Lettr., 42, 486 (1979).

26. D. Antreasyan et al, CERN Report, EP/79-116, (1979).

27. T. Toohig, Fermilab Magnets, Power Supplies, and Auxiliary Devices: Technical Data, Fermilab TM-632, (1975).

28. D. C. Carey, TURTLE (Trace Unlimited Rays Through Lumped Elements), Fermilab TM-64, (1971).

FERMILAB HIGH INTENSITY LABORATORY SPECTROMETER

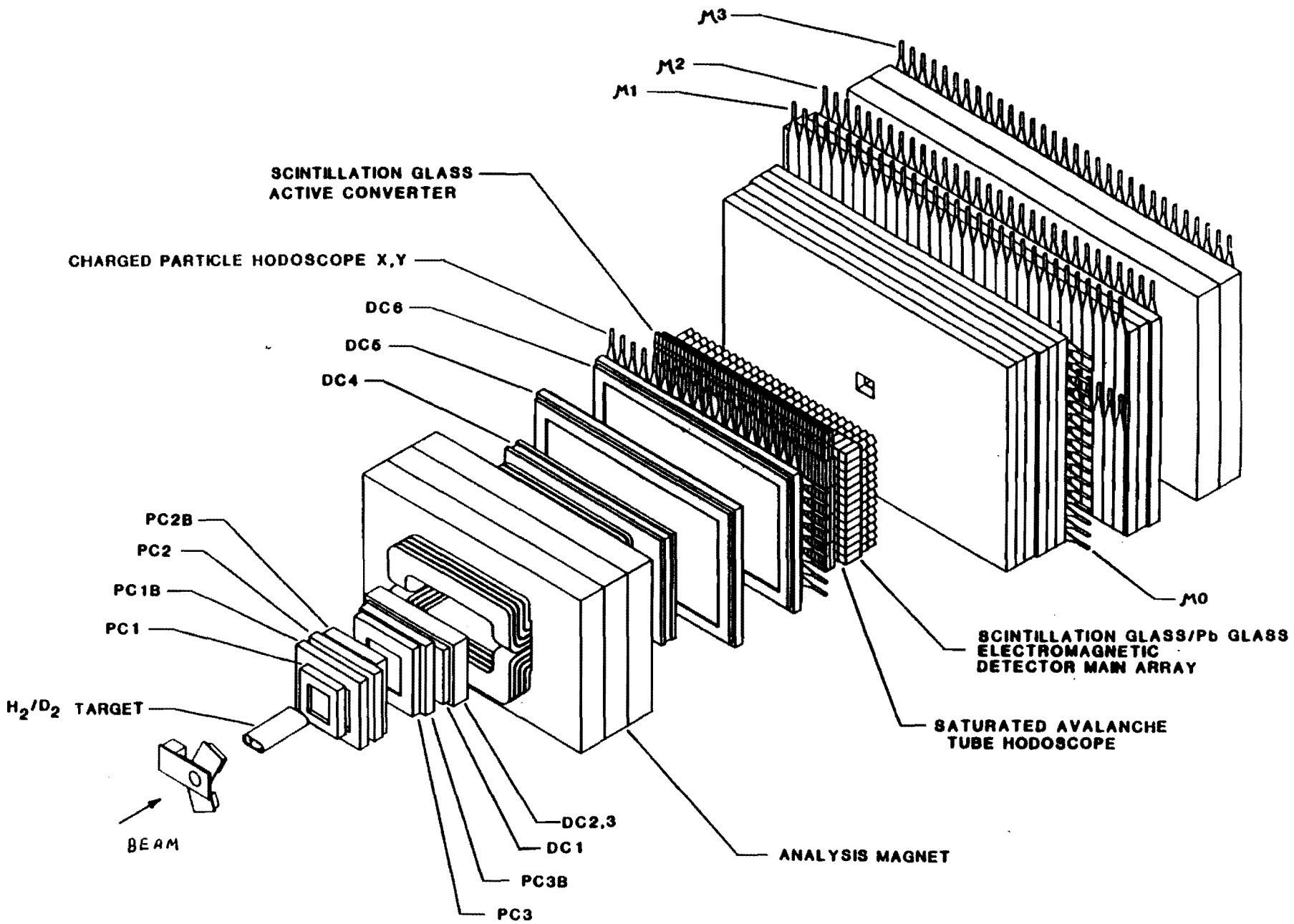

Fig. 1

P771 W Target and Silicon Tracker

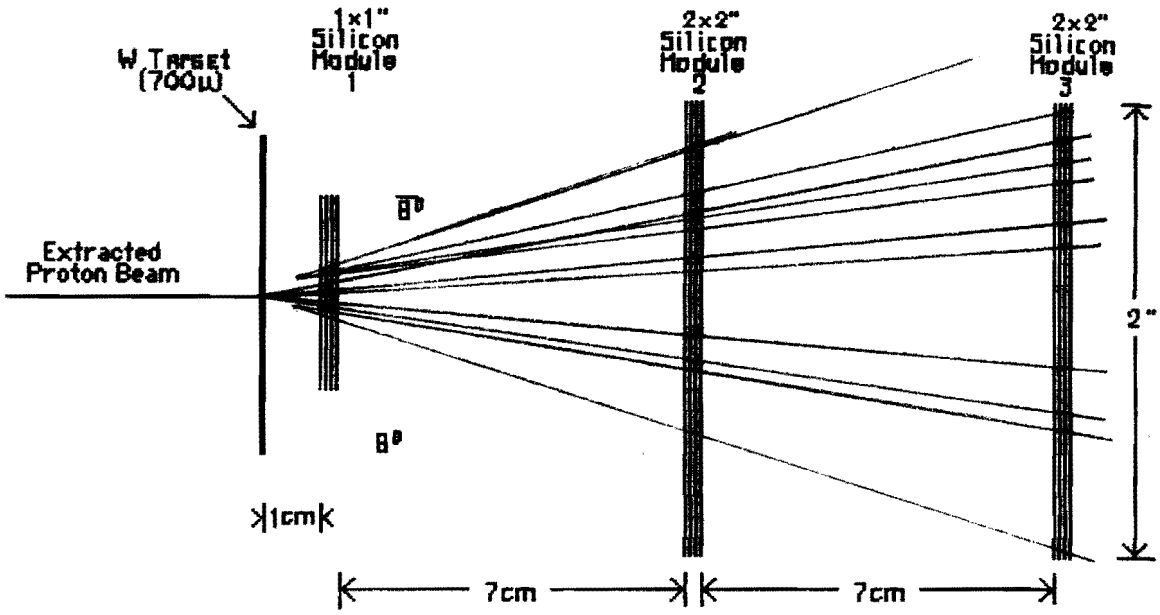

Fig. 2 Tungsten target and silicon tracker configuration for P771. Each silicon tracker module consists of an x,u,v,x′ set of 300 micron silicon planes with 50 and 100 micron strips. Shown superimposed on the tracker is a $B^0\overline{B}^0$ event. The orientations of the u,v planes are nominally at 16.7^0 with respect to the x and x′ planes.

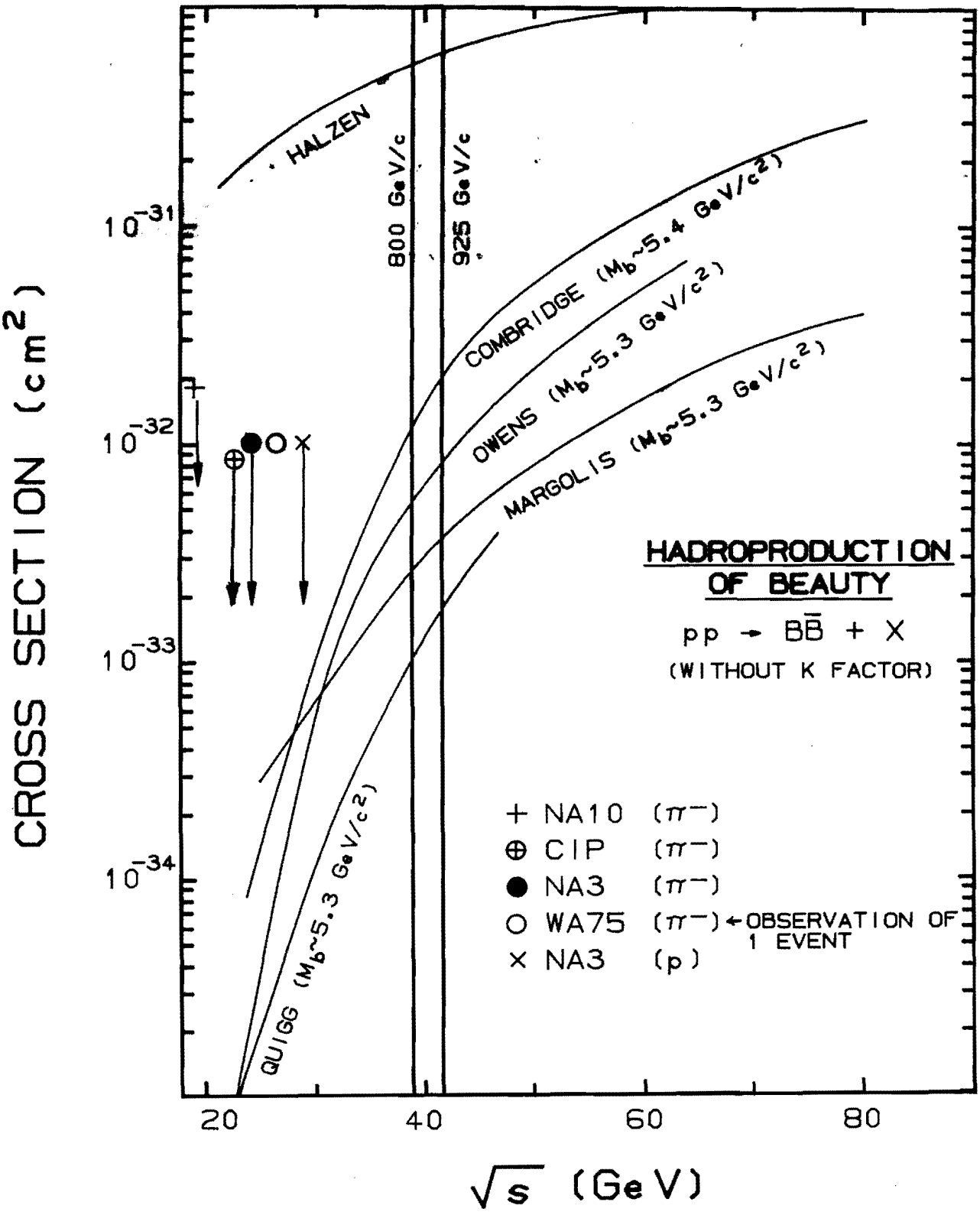

Fig. 3 Proton-proton cross sections for hadroproduction of beauty as predicted by several calculations. The experimental data consists of upper limits. The only direct observation of beauty reported thus far is the observation of a $B\bar{B}$ pair in one event by WA75.

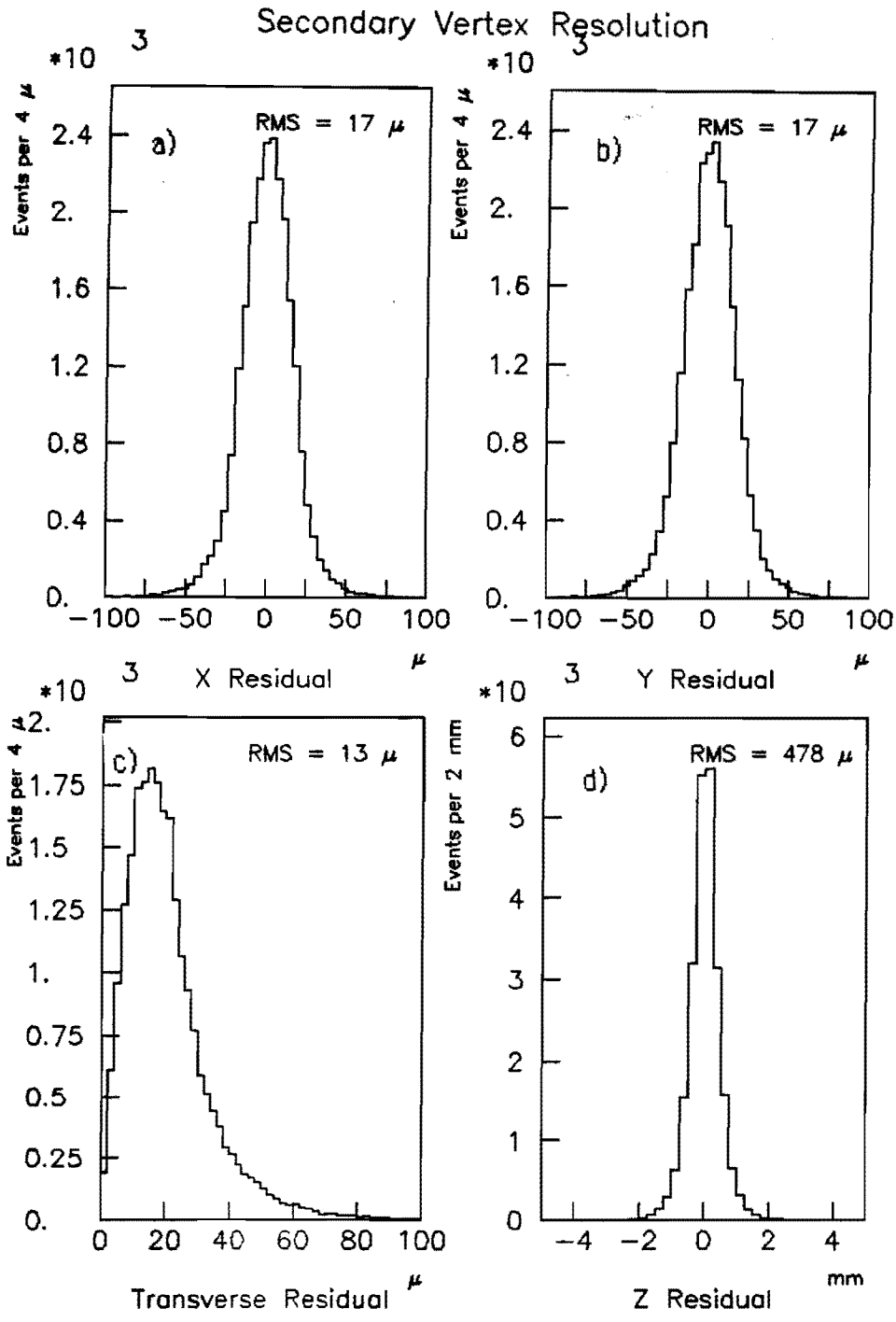

Fig. 4 Residuals of the beauty meson decay vertex as reconstructed from the $\psi \rightarrow \mu\mu$ tracks in the decay $B \rightarrow \psi K\pi$. The transverse residuals Δx, Δy, $\Delta r = \sqrt{\Delta x^2 + \Delta y^2}$ and the Δz residual along the beam direction are calculated with respect to the true coordinates of the decay points.

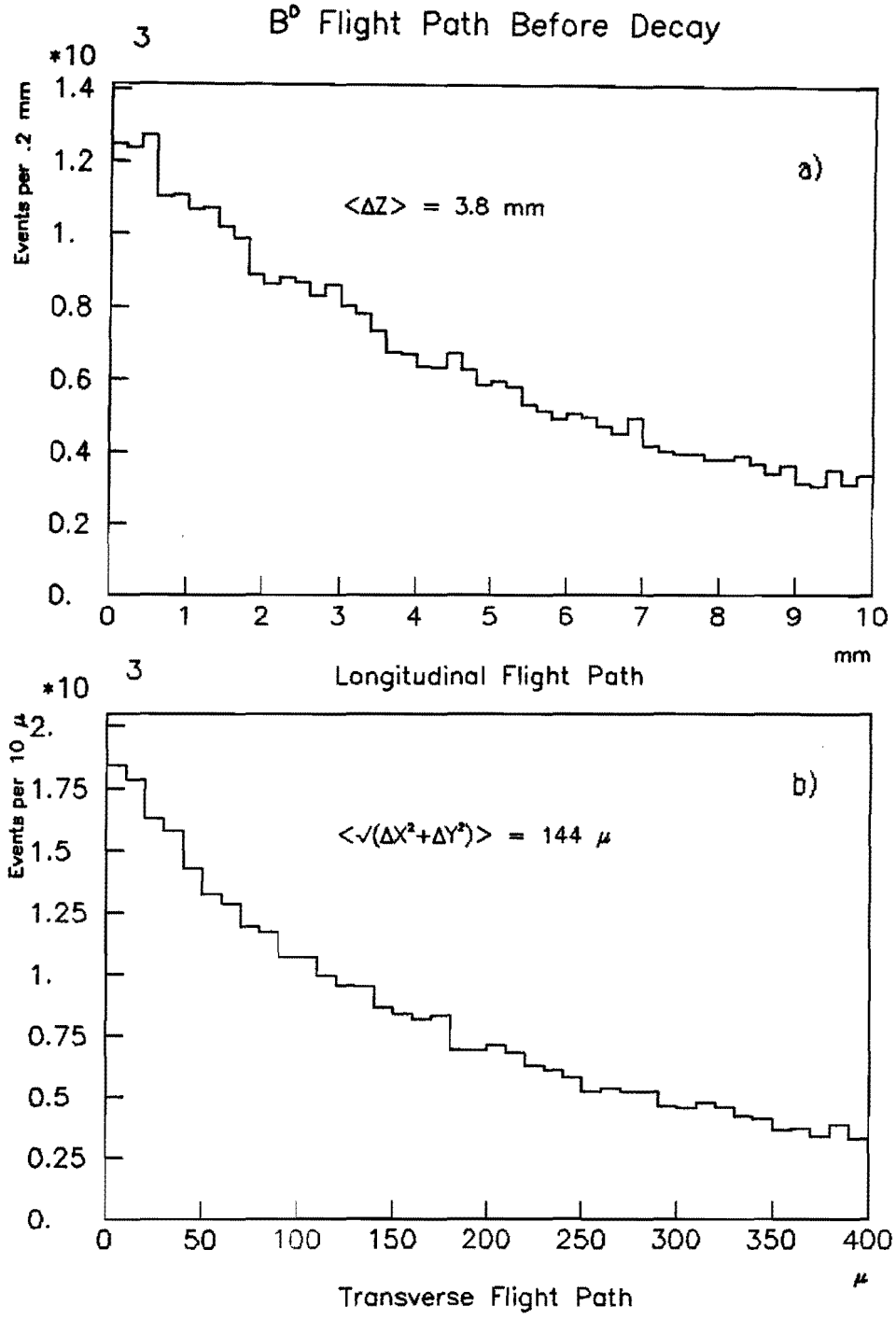

Fig. 6 B^0 flight distances before decay calcculated relative to the true B^0 production point. a) the longitudinal distance along the beam direction. b) the transverse distance from the production point.

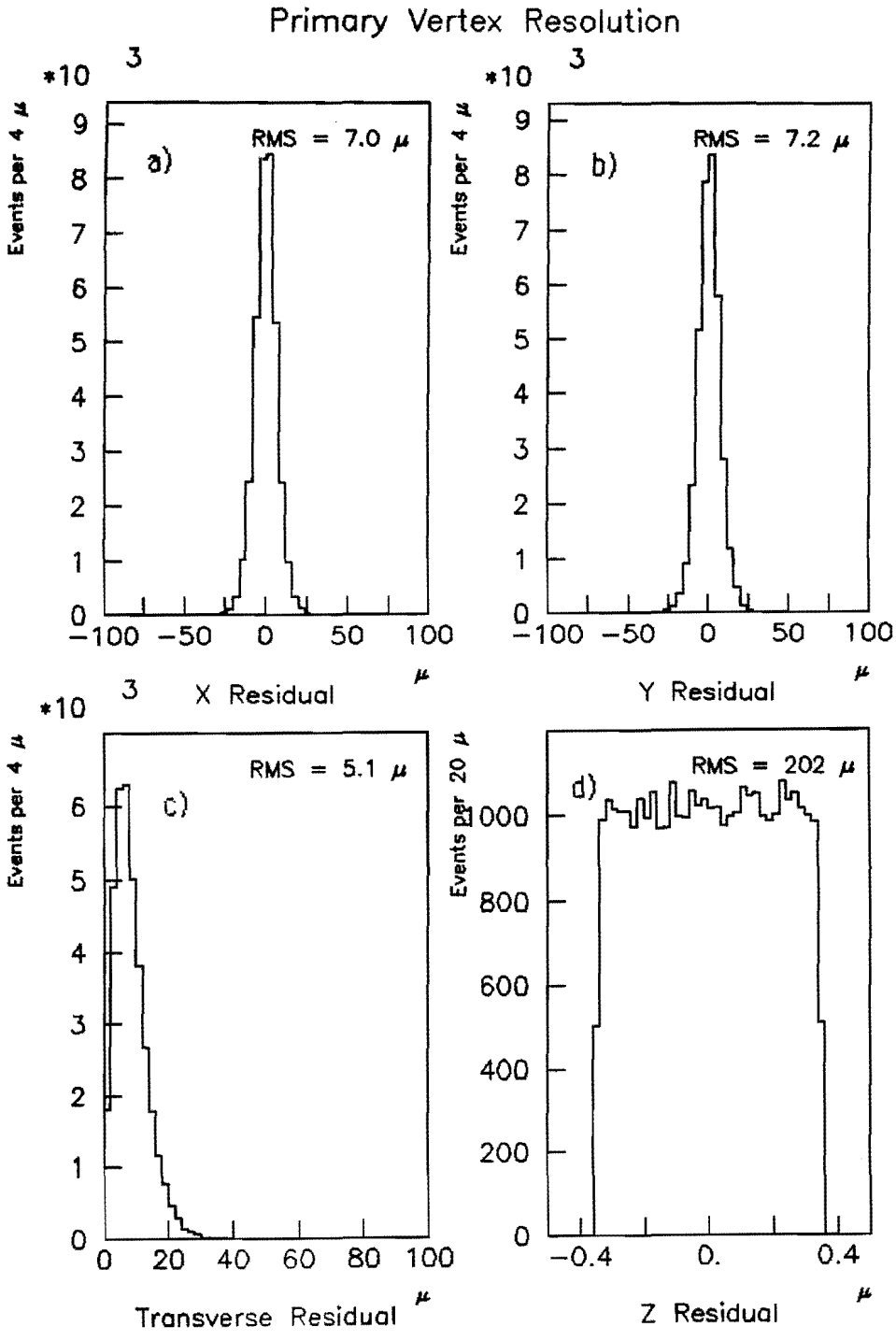

Fig. 6 Primary vertex residuals relative to the true primary production point.

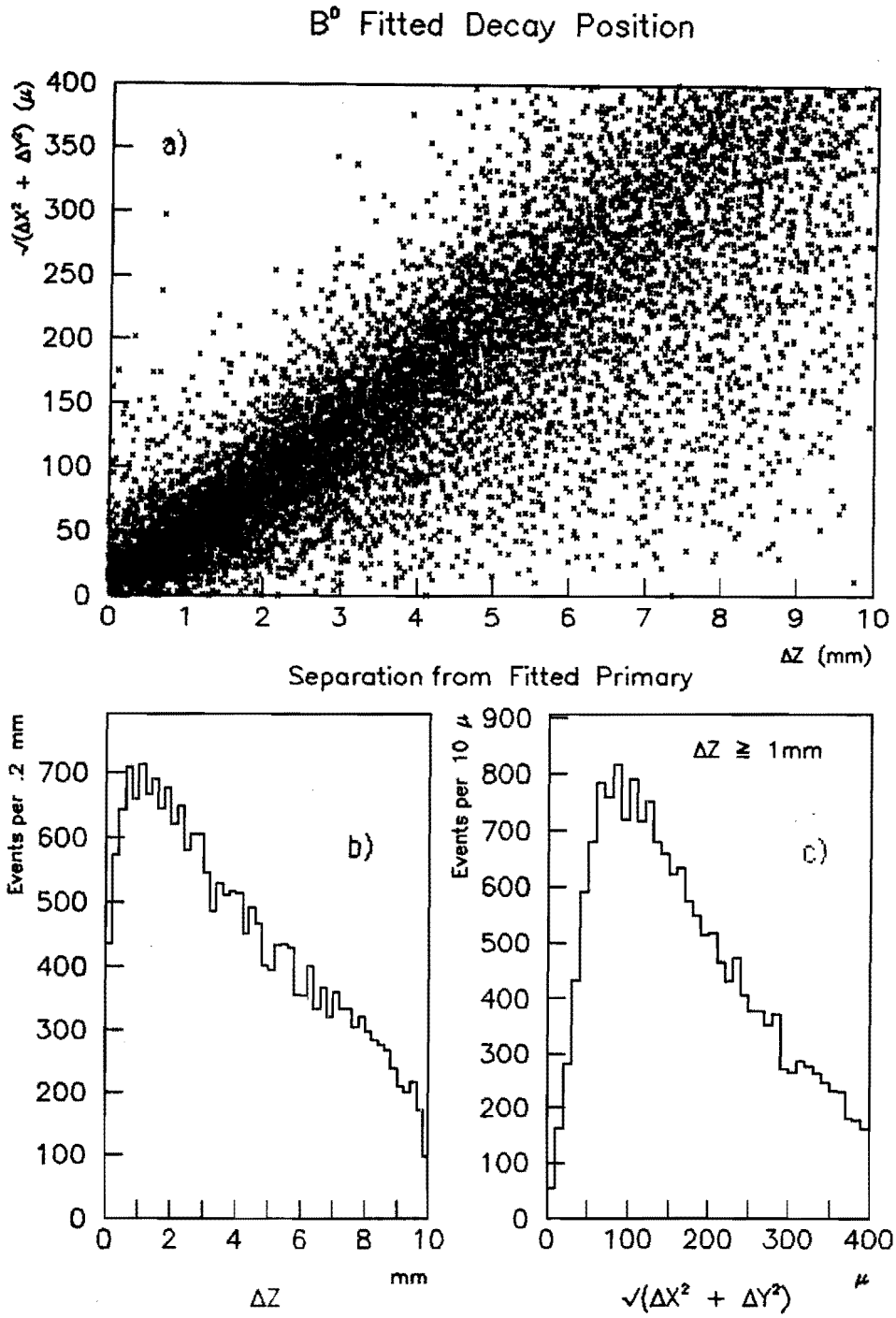

Fig. 7 a) Scatterplot of $\Delta r=\sqrt{\Delta x^2+\Delta y^2}$ vs Δz for the separation of the B^0 decay vertex (formed from the $\psi \longrightarrow \mu\mu$) relative to the fitted primary vertex. b) Δz projection c) Δr projection

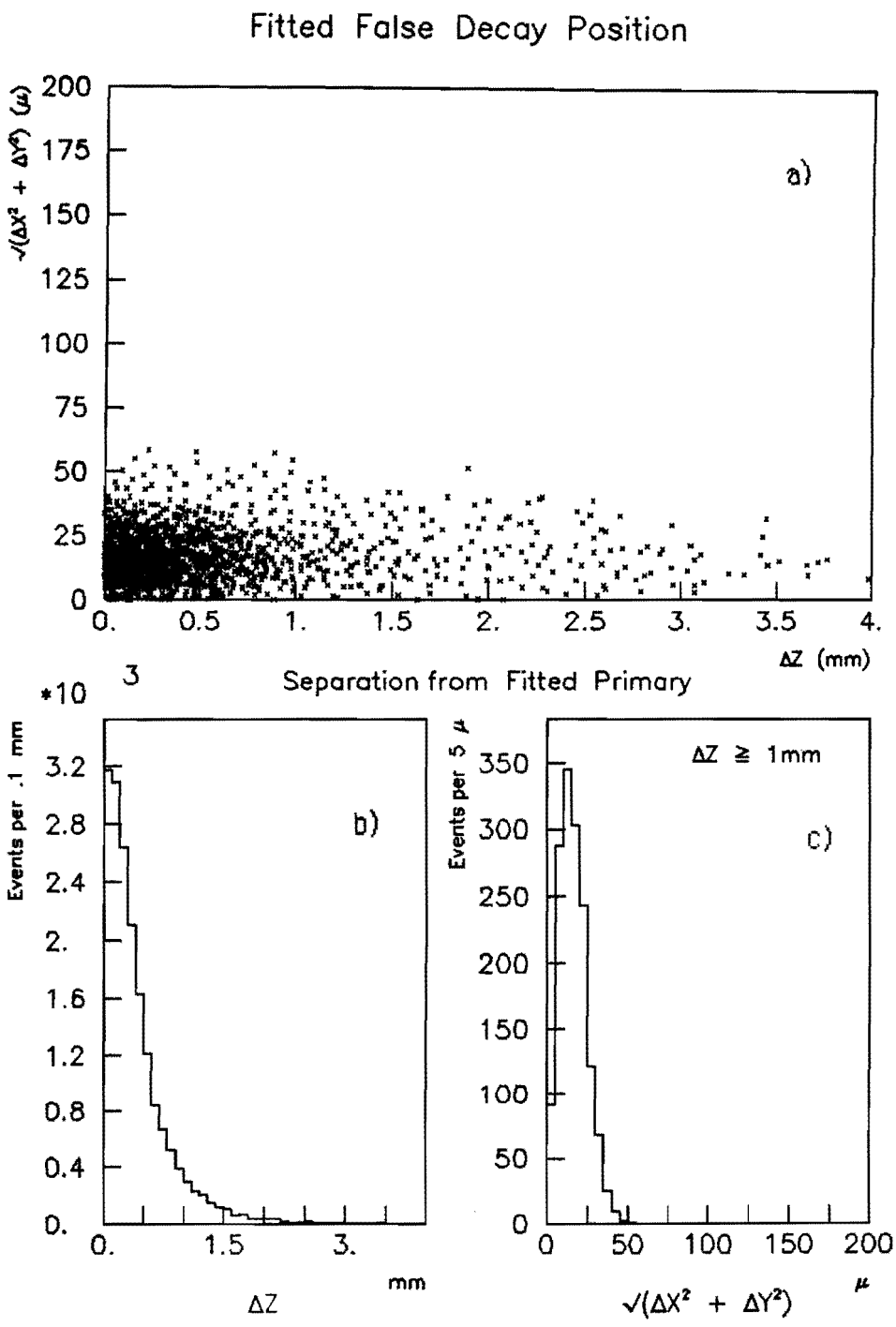

Fig. 8 a) Scatterplot of Δr vs Δz for the separation of vertices reconstructed from "ordinary" Ψ's produced at the primary vertex relative to the fitted primary vertex. b) Δz projection c) Δr projection

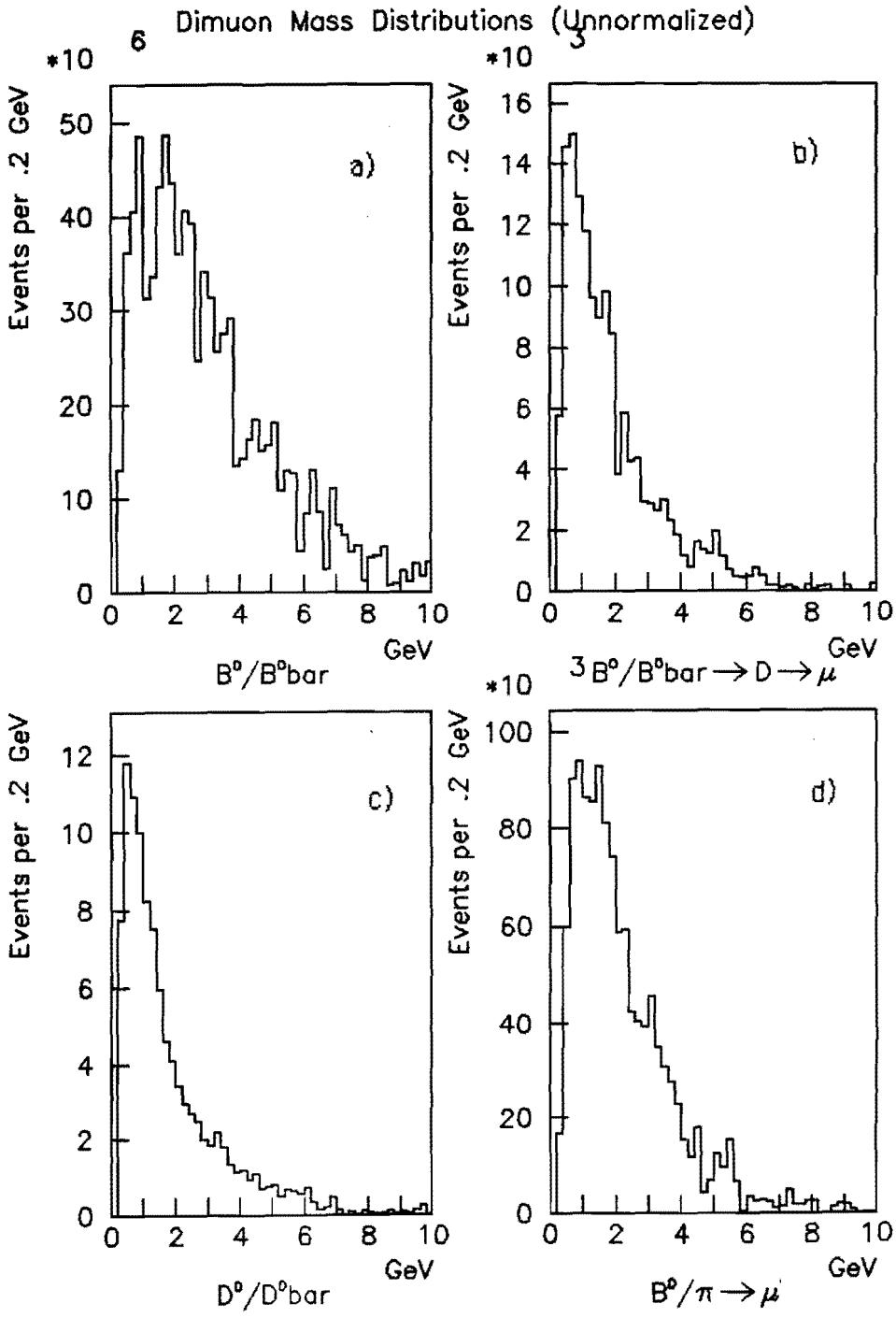

Fig. 9 Same sign dimuon mass distributions for a) $B^0\overline{B}^0$ mixing signal b) background from B—>D—>μ "charmed daughter" decays c) background from $D^0\overline{D}^0$ mixing d) background from B—>π—>μ decays. Notice that the three backgrounds are more peaked at low mass than the $B^0\overline{B}^0$ signal.

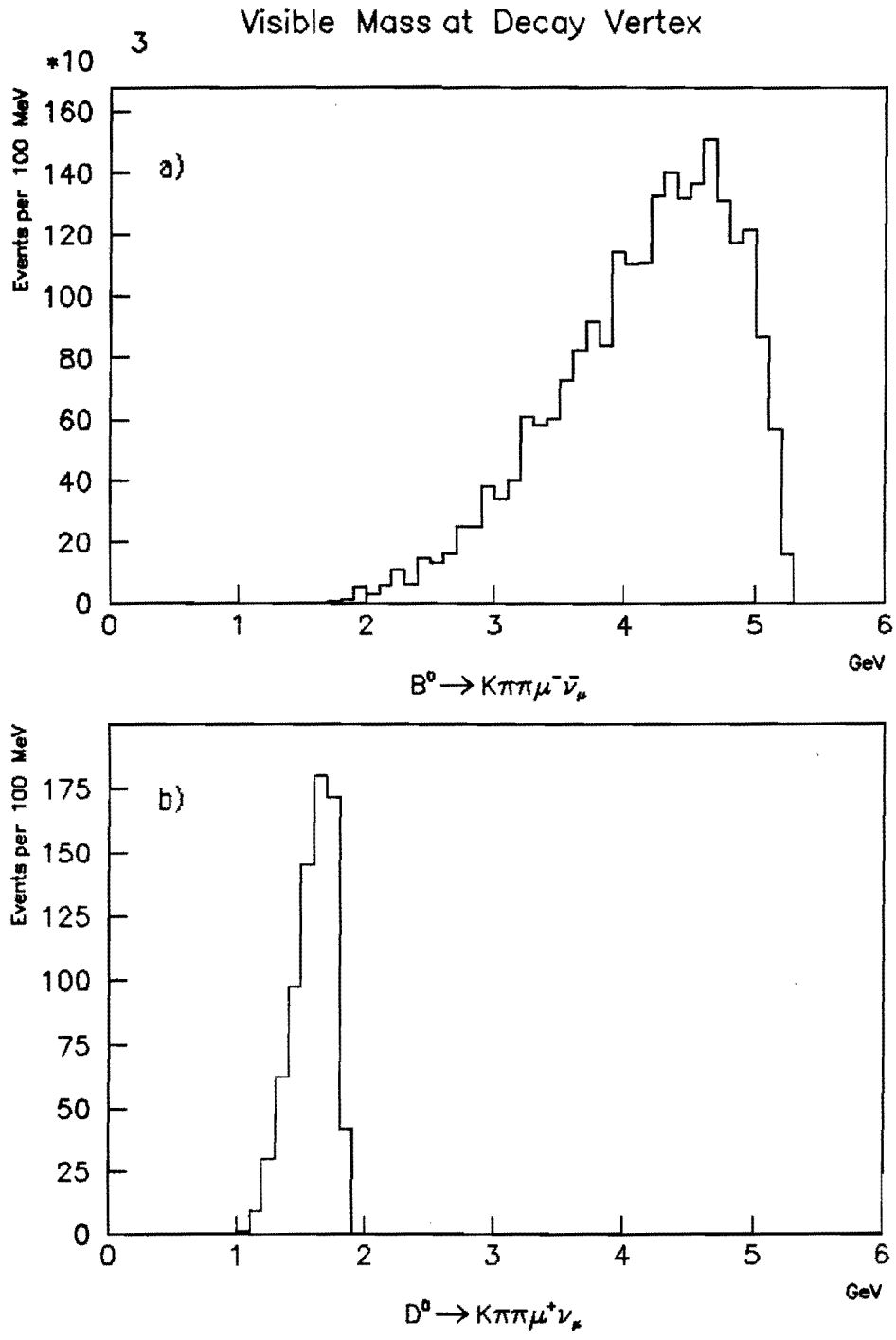

Fig. 10 Visible mass for the a) B—→Kππμν and b) D—→Kππμν decays with 100% correct assignment of tracks to the secondary vertex.

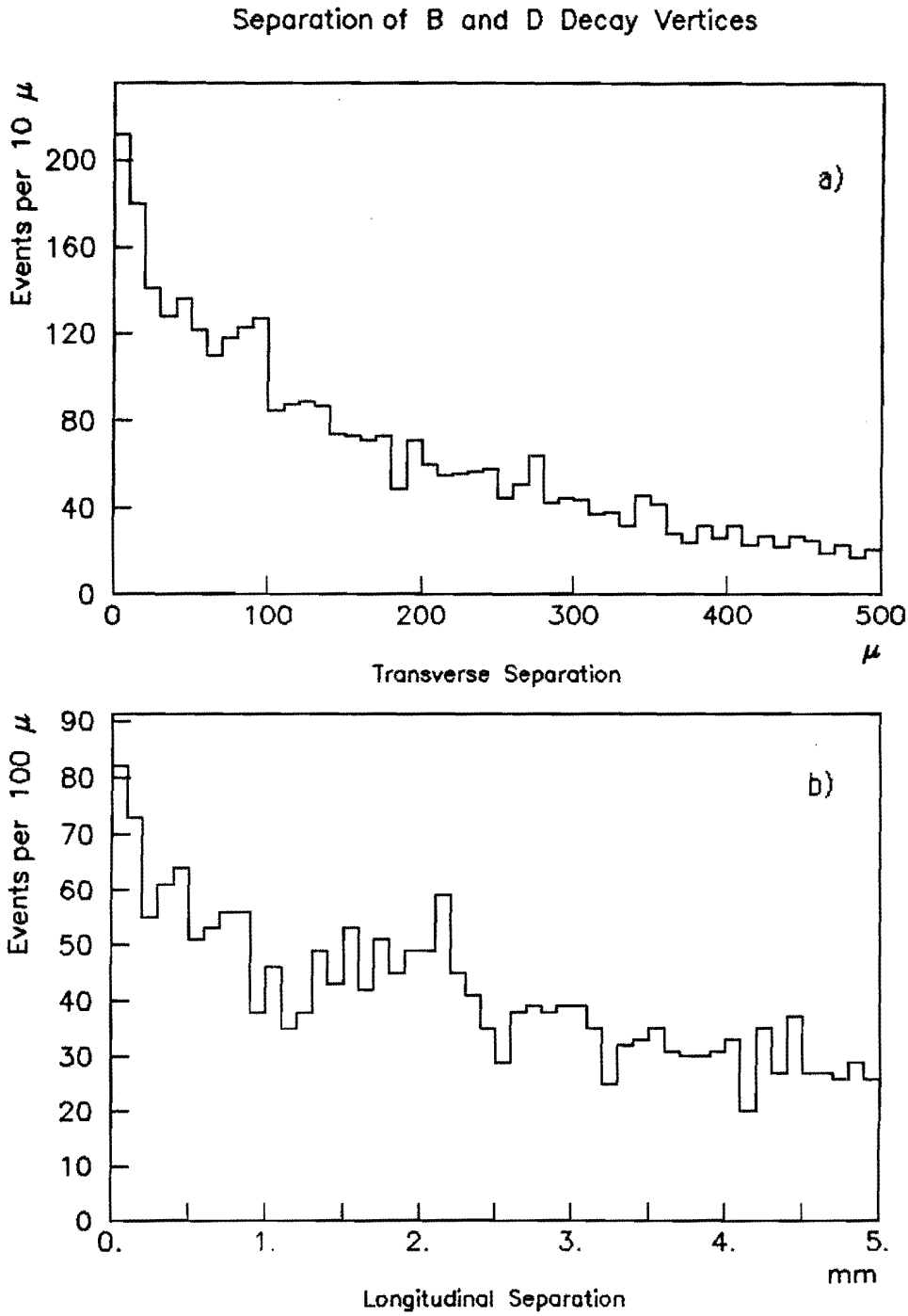

Fig. 11 Separation of the true B and D vertices in the sequential decays B→D in the a) r and] z coordinates.

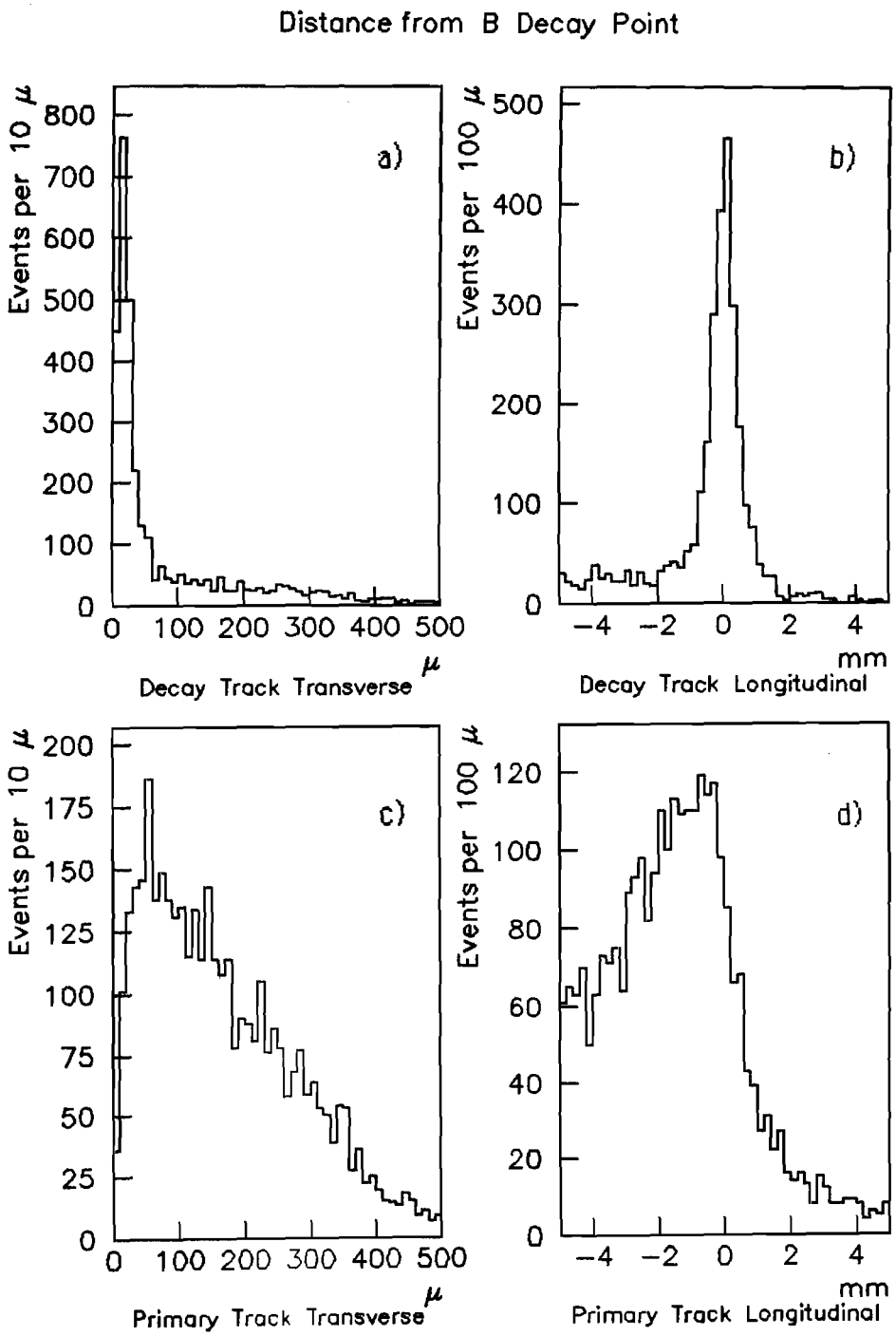

Fig. 12 Distances a) Transverse and b) Longitudinal between the midpoint of the shortest cord between a decay muon and a decay track and the true decay point. c) and d) Same quantities for the primary tracks.

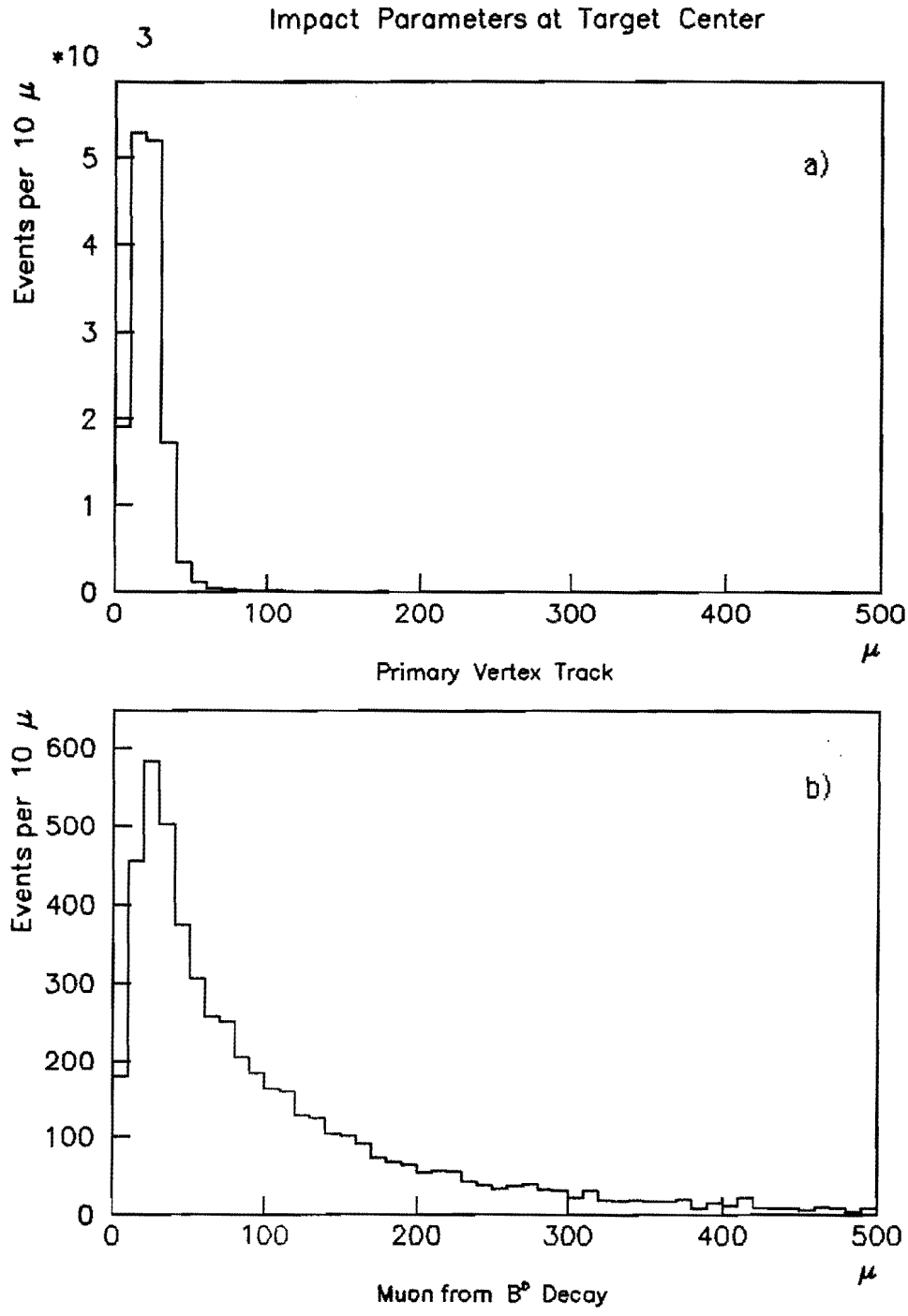

Fig. 13 Transverse distance of the a) tracks from the primary vertex b) muons from the secondary decay vertex from the primary vertex as calculated at target center.

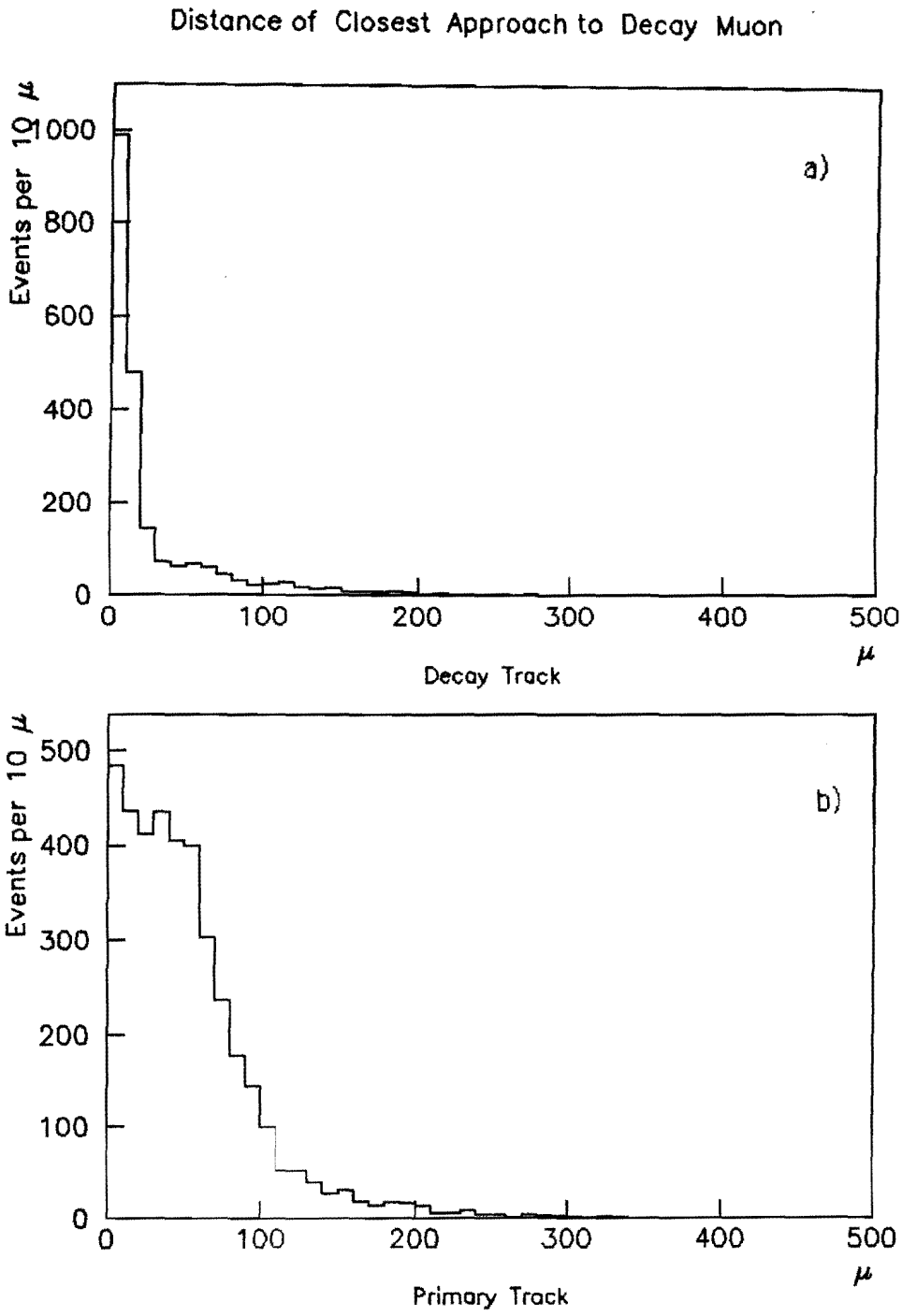

Fig. 14 Length of the shortest line segment linking a track to the B decay muons for a) B decay tracks b) primary tracks.

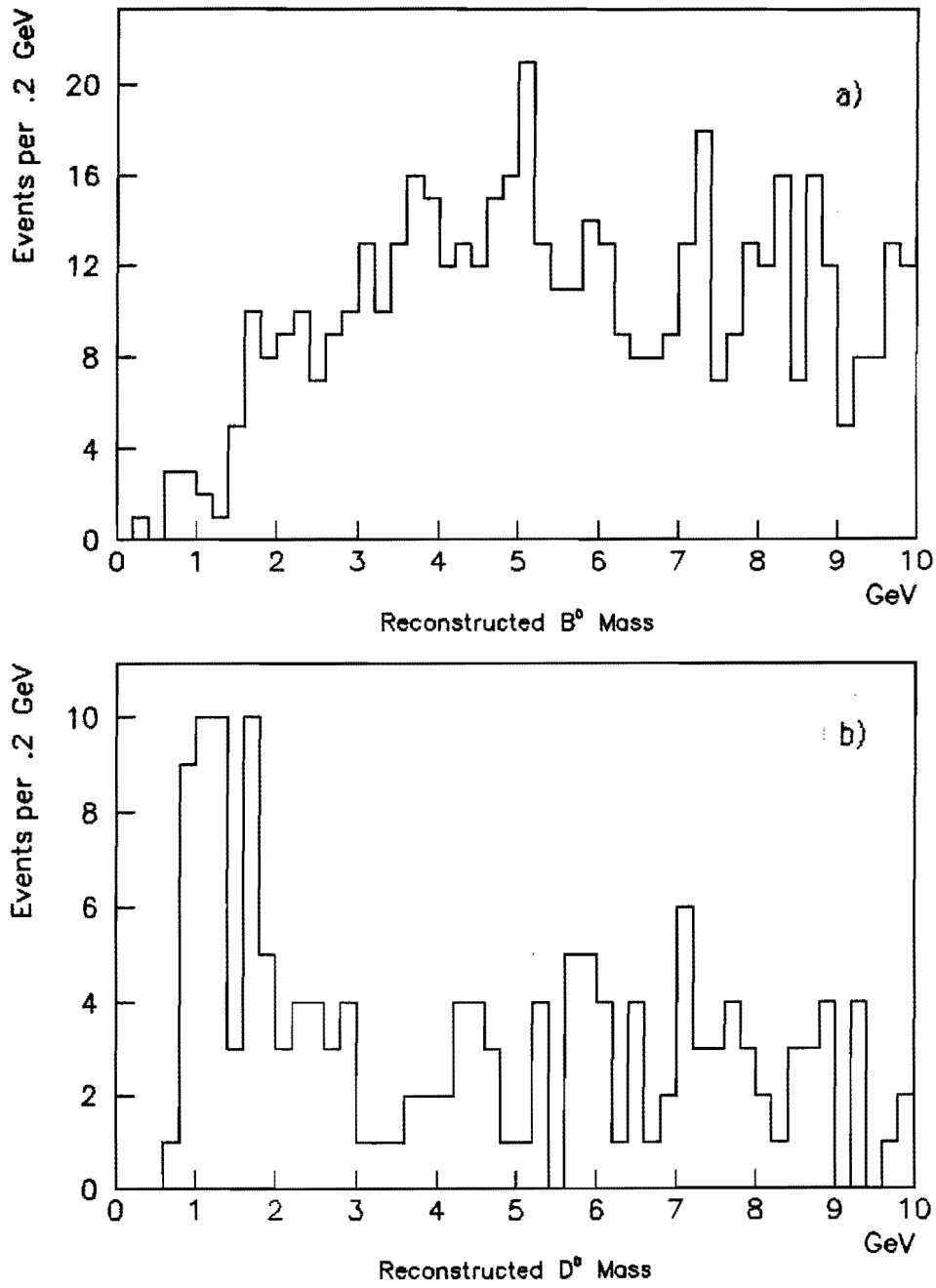

Fig. 15 Visible mass for a) $D \rightarrow K\pi\pi\mu\nu$ decays b) $B \rightarrow K\pi\pi\mu\nu$ decays as reconstructed using the strategy for track assignment for secondary and primary vertices discussed in the text.

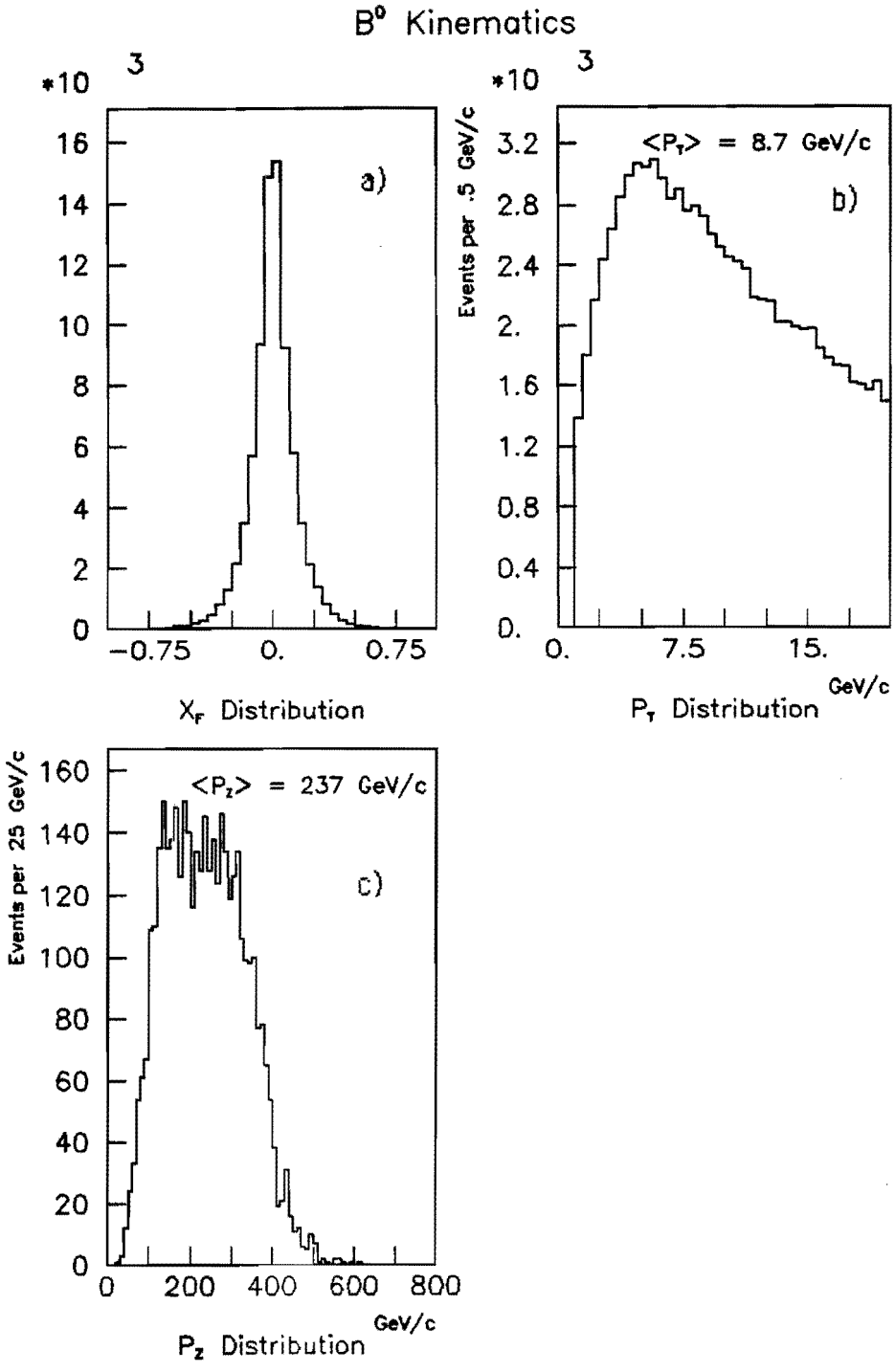

Fig. 16 a) x_F b) p_t and c) p_z distributions of B's generated using the model of Appendix B.

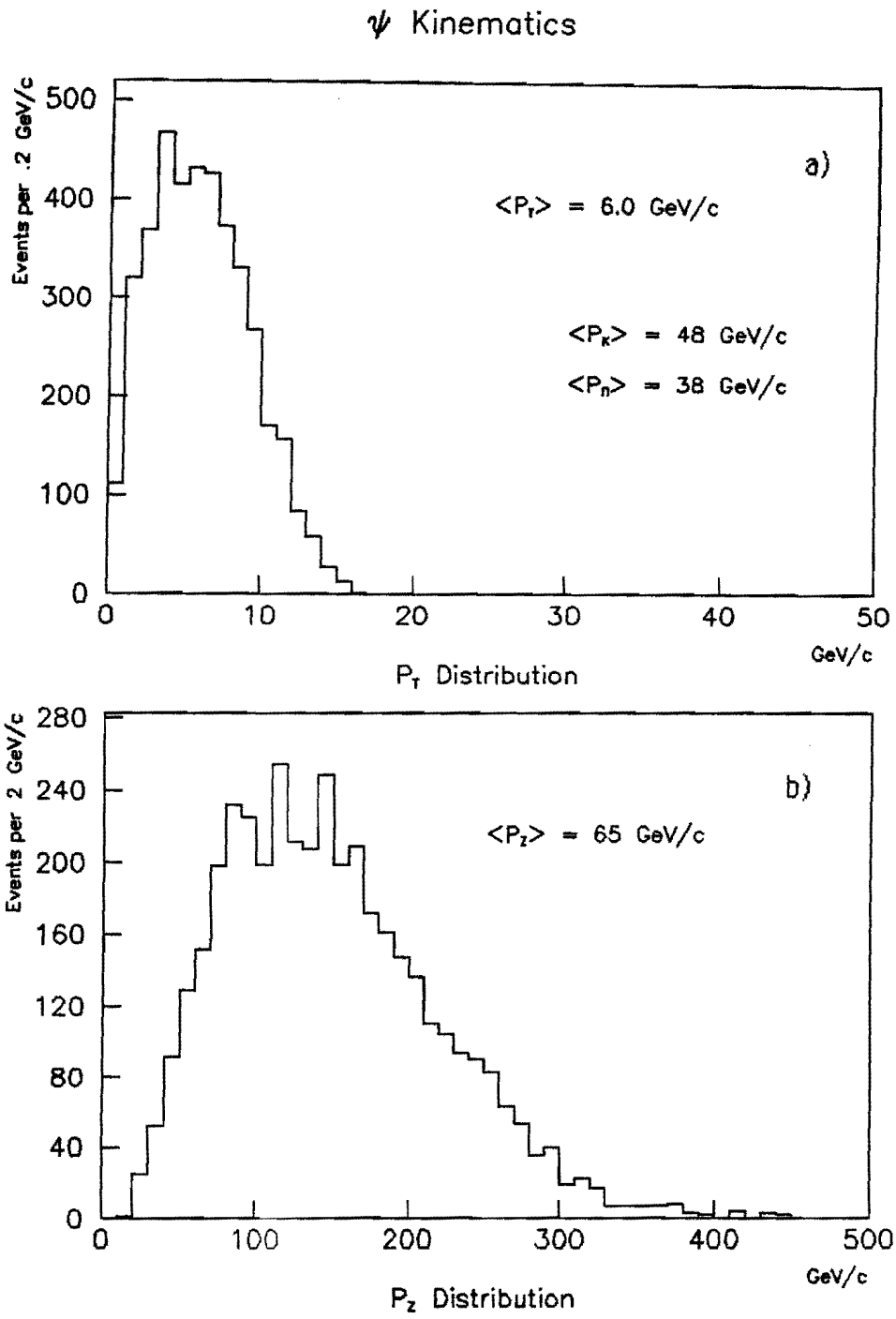

Fig. 17 a) p_t and b) p_z distributions for ψ's from the decay $B \rightarrow \psi K\pi$ generated using the model of Appendix B.

Attached are corrected pages 3, 7, 9, 17, 18, 19, 20, and 21 for P-771 (Cox).

B_{du} , B_{us}, B_{ds} , etc. which can also decay into ψ + anything. Beauty quark baryon production, however, by analogy with light quark baryon production is expected to be less copious than beauty meson production.

The experimental signature for such physics will be events with opposite sign dimuons which point at a secondary decay vertex as measured by the silicon tracker where the muon pairs reconstruct to the ψ mass. The association of the ψ with a secondary decay vertex insures that one is seeing beauty rather than charm production. Since the branching ratio for B —> ψ + anything has been measured by both the ARGUS[7] (1.10±0.19%) and CLEO[8] (1.10±0.21±0.23%) experiments and a rough lifetime for beauty is known ($3.0\pm_{1}^{2}\times10^{-13}$ sec for the WA75 measurement[9], $1.2\pm0.2\times10^{-12}$ sec for the PEP-PETRA measurements[10,11]), it is possible to determine the cross section for beauty hadroproduction from our observation of associated with secondary vertices without complete reconstruction of the beauty meson final states.The calculation of the cross section without complete reconstruction of particular final states will depend to a small extent on a model dependent estimate of the efficiency for seeing the secondary vertex. Background to the detection of beauty decay comes primarily from "ordinary" ψ production in which the ψ fakes a secondary vertex by reconstructing to a point far from the primary vertex because of measurement errors .

B) In addition to the observation of B —> ψ + anything and the inference of the total cross section for beauty meson production, we intend to reconstruct specific exclusive final states of the beauty mesons containing ψ's. Complete reconstruction of particular exclusive final states permits the direct measurement of momentum and lifetime distributions and provides extra constraints for the measurement of the hadroproduction cross sections for beauty. This complete reconstruction will be possible for some final states. We list in Table I the Cabibbo favored final states for some of the beauty meson decays that result in less than or equal to four charged particles. Estimated branching ratios[12] are provided in some cases and in one particular case ($B\longrightarrow\psi K^{-}$) an experimental measurement[13] is available. The antimeson decay table is similar of course except for CP violating effects. We note that the B^0, $\overline{B^0}$ secondary vertices result in an even number of outgoing charged tracks

at 300 GeV/c. At the same time as we perform the search for beauty production, we would continue the study of charmonium production at the higher energy using the 800 -> 925 GeV/c primary proton beam to measure χ production from the heavy target:

$$\begin{array}{l} p\ W \longrightarrow \chi + \text{anything} \\ \qquad\quad \hookrightarrow \gamma\ \psi \\ \qquad\qquad\quad \hookrightarrow \mu^+\mu^- \end{array} \qquad (4)$$

The measurement of energy dependence of charmonium production will allow us to more completely determine the production mechanisms and the gluon structure function of the nucleons. (see Ref. 1)

E) Finally, using the primary proton beam at the highest energy we plan to search for evidences of hadronic production of χ_Υ in much the same way that we are measuring charmonium production, i.e.:

$$\begin{array}{l} p\ W \longrightarrow \chi_\Upsilon + \text{anything} \\ \qquad\quad \hookrightarrow \gamma\ \Upsilon \\ \qquad\qquad\quad \hookrightarrow \mu^+\mu^- \end{array} \qquad (5)$$

IV. Beam Requirements/Experiment Running Requirements

We are basing our estimates of yields on a canonical run of 20 weeks of beam. We anticipate **2.8×10^6 seconds of beam** (20 weeks×100 hours/week×60min/hour×23 seconds of spill/min). We will use the primary proton beam to take advantage of the maximum energy available (800—>925 GeV/c). The scheme for the upgrade of the P-West High Intensity Laboratory secondary beam line is straightforward and is detailed in Appendix A. We will require **1.7×10^8 protons per second** of spill or **$\approx3.9\times10^9$ protons per spill** during data taking. This beam intensity implies a total interaction rate of **2×10^6 interactions per second** from our target and our silicon tracker assuming the use of the 700 micron W target described below. Approximately **1×10^6 interactions per second** are generated by each of these devices. We

Finally, as in experiment E-705, we will require occasional use of the calibration electron beam for adjustment of our electromagnetic detector. We summarize in Table I below the expected beam usage and the spot sizes that we expect on the experiment target.

Table II

Proton Beam	Max Flux/sec	Flux/spill(23 sec)	σ_x(cm)	σ_y(cm)
800-925 GeV/c	1.7×10^8	3.9×10^9	0.2	0.2

V. Experimental Setup

A) General Remarks

We plan to use the E-705 spectrometer (Figure 1) augmented by a silicon tracker and a W foil target (Figure 2). We will take advantage of the multi-stage dimuon trigger which has been developed for this spectrometer and has already been used in experiment E-537 and is currently being used in experiment E-705. This trigger, which includes an ECL-CAMAC trigger processor[2,3] which forms an dimuon mass in < 10 μs from the muon candidate tracks that it finds in the spectrometer's drift chamber system, presently provides a suppression of $<10^{-4}$ of the interactions due to the total cross section. When this trigger is coupled to our data acquisition system which is capable of handling 200 events/sec, we will operate in P771 at an interaction rate of 2×10^6 interactions per second producing 100 dimuon triggers/second from the target. This is a more comfortable manner of operation than that of E705 which requires that we operate at 200 triggers per second in the absence of filtering.

B) W Foil Target

We have chosen to use a 700 microns thick tungsten foil. Tungsten has been chosen as the target material in spite of the relatively large ratio of interaction length to radiation length for two main reasons:

1. The density of tungsten allows a relatively thin foil for a given number of interaction lengths and minimizes the number of secondary

The signal for this physics is same sign dimuons where each muon comes from a different secondary vertex. The B^0 or $\overline{B^0}$ evolve into one another and then decay semileptonically thereby producing a same sign dimuon signal:

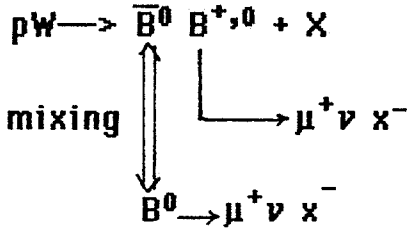

The semileptonic branching ratio for $B_{u,d}$—>μ+ν+hadrons is 12.4%. We assume that this branching ratio is approximately the same for B_s. If we look for the simultaneous semileptonic decay of both the B's to detect $B^0\overline{B^0}$ mixing, we will observe 1.54×10^{-2} of all produced $B\overline{B}$ final states undergoing double semileptonic decay and producing opposite sign dimuons. If some of the B^0's evolve into their antiparticles then we will observe a same sign dimuon signal which is some fraction of this opposite sign dimuon signal. It is expected[20,21] that the majority of mixing occurs between $\overline{B^0}_s$ and B^0_s. The expected level of the mixing of the strange beauty meson is approximately[20,21] 20%. If B_d, B_u and B_s are produced equally copiously in the hadronization of the b quarks in pN interactions, then 4/9 of the possible $B\overline{B}$ final states will include one B^0_s meson that can evolve into a $\overline{B^0}_s$ meson and 1/9 of the final $B\overline{B}$ states will have two B^0_s mesons. Therefore,we would expect to see a like sign dimuon signal due to $B^0\overline{B^0}$ mixing which is 1.89×10^{-3} of all $B\overline{B}$ final states. The geometric acceptance for muons from double semileptonic decays of beauty has been estimated to be 25%. So we expect to see between 425 and 5200 same sign dimuons from mixing in comparison to the 3500 to 42400 opposite sign dimuon from the double semileptonic decays of B's produced in 800 GeV/c interactions depending on the cross section for beauty. For 925 GeV/c pW interactions we would expect to observe between 660 and 8100 same sign dimuons from mixing in comparison to 8200 to 40500 opposite sign dimuons.

The backgrounds to $B\bar{B}$ mixing come from several sources. The most serious background is produced by the sequential decay of one of the B's to a charmed daughter which decays semileptonically into a muon with opposite sign to that produced by the semileptonic decay of the parent B. This will produce a same sign dimuon background if the other B also decays semileptonically. There are several decay chains which result in this sort of "daughter charmed particle" same sign background. Under the assumptions 1) that B_u, B_d and B_s are made equally frequently and 2) that the various reported branching ratios (the ratios that are used are either preliminary results from the CLEO experiment[22] or reported ratios from the particle data tables[23]) for decays of unseparated mixtures of $B_d^0, \bar{B}_d^0, B_u^+, B_u^-$ can be used both for the individual beauty mesons and for B^0_s mesons, we can evaluated the backgrounds due to the decay sequences listed below. We have allowed in these calculations for the mixing of B^0_s and $\bar{B}^0_s$ which reduces any background produced by final states containing B_s.

1. Charged B plus neutral B production followed by decay of $B^{\pm} \rightarrow D^{\bar{0}}, ^0$:

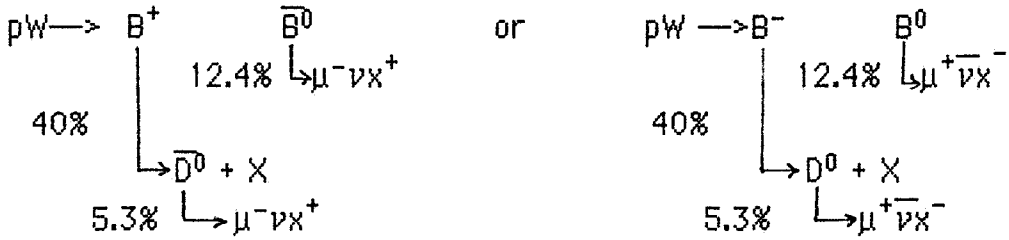

Thus, 2.6×10^{-3} of the $B^+\bar{B}^0 + B^-B^0$ production (4/9 of all $b\bar{b}$ pairs) decays via this route producing 230 to 2900 same sign diμ in a 800 GeV/c run.

2. Charged B plus neutral B production followed by decay of $B^{\pm} \rightarrow D^{\pm}$:

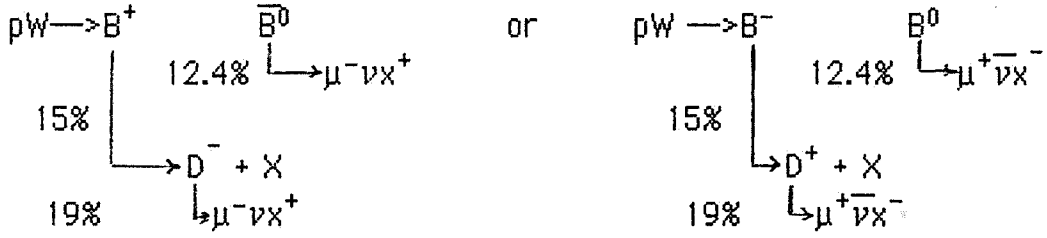

An additional 3.5×10^{-3} of the $B^+\overline{B^0}$ + B^-B^0 production (4/9 of all $b\overline{b}$ production) will decay via charged D's into a same sign dimuon background of 315 to 3900 events in the 800 GeV/c run.

3. Charged B plus neutral B production followed by decay of $B^{0,\overline{0}} \rightarrow \overline{D^0}, D^0$

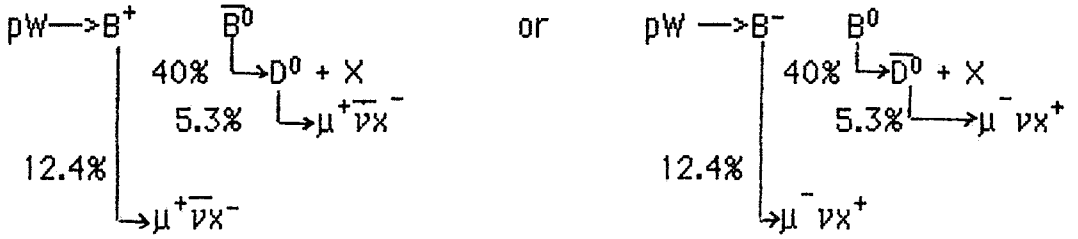

This decay chain is responsible for an additional 2.6×10^{-3} of the $B^+\overline{B^0}$ $+B^-B^0$ production decaying to a same sign background of 230 to 2900 events

4. Charged B + neutral B production followed by decay of $B^{0,\overline{0}} \rightarrow D^-, D^+$

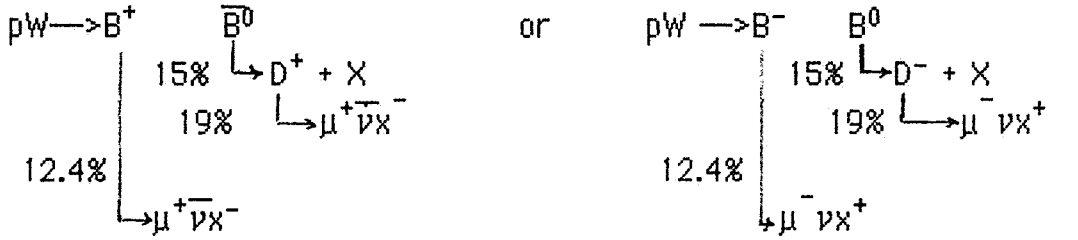

Finally, this decay chain is responsible for an additional 3.5×10^{-3} of the $B^+\overline{B^0}$ $+B^-B^0$ production decaying to a background of 315 to 3900 events.

5. Neutral B production followed by decay of $B^{0,\overline{0}} \rightarrow \overline{D^0}, D^0$

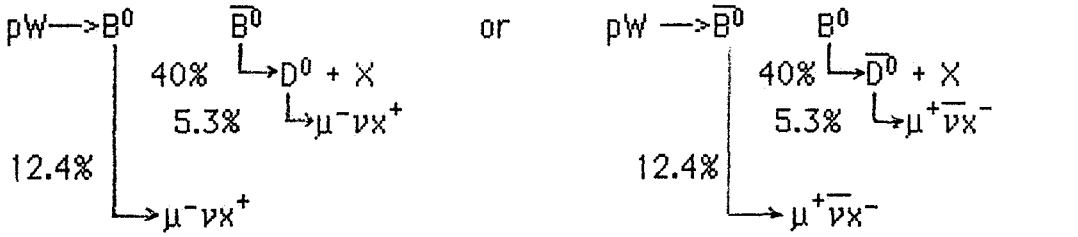

This decay sequence results in 2.6% of the $B^0\overline{B}^0$ final states (4/9 of the total $b\overline{b}$ production) decaying into a same sign background which contains 240 to 2950 events for the 800 GeV/c run.

6. Neutral B production followed by decay of $B^{0,\overline{0}} \rightarrow D^-, D^{\pm}$

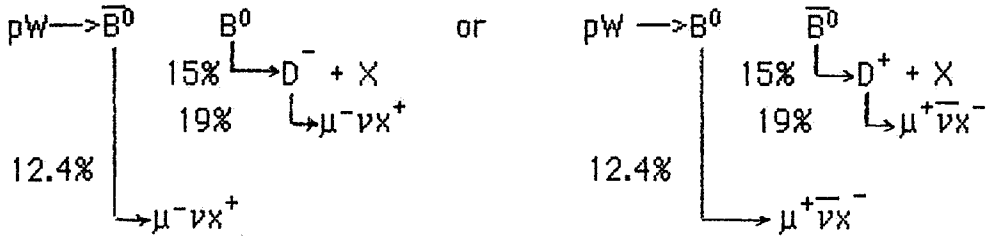

3.5×10^{-3} of the $B^0\overline{B}^0$ production (4/9 of the entire $b\overline{b}$ production) decays via this chain to a same sign dimuon background of 320 to 3950 events.

7. Charged B production followed by decay of $B^{\pm} \rightarrow D^{\pm}$

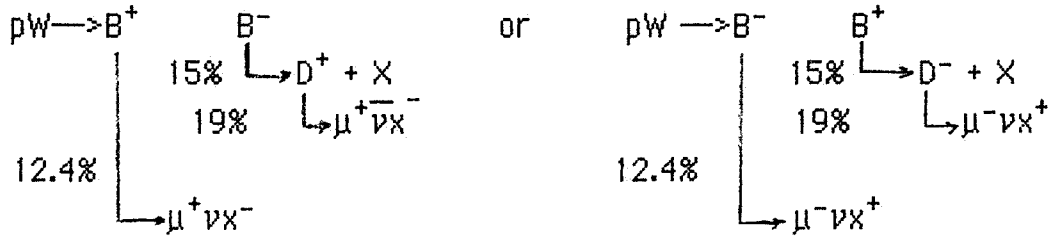

3.5×10^{-3} of the B^+B^- final states (1/9 of all $b\overline{b}$ final states) decay via this sequence to a same sign muon background of 90 to 1070 events.

8. Charged B production followed by decay of $B^{\pm} \rightarrow \overline{D}^0, D^0$

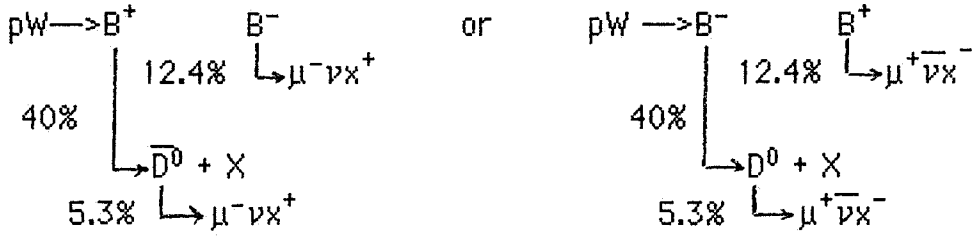

2.6×10^3 of the B^+B^- final states (1/9 of all $b\bar{b}$ final states) decay via this sequence producing a same sign muon background of 70 to 800 events.

Thus, the total same sign background from the sum of these sequences, in the absence of any cuts to suppress them, would be 1800 to 22400 events to be compared to a $B^0\bar{B}^0$ mixing signal of 425 to 5200 events in an 800 GeV/c run. So our signal to background is 1/4 from the charmed daughter decay sequences without cuts.

The second same sign background to $B\bar{B}$ mixing is production of $D^0\bar{D}^0$ followed by mixing and the subsequent semileptonic decay of the charmed particles. In this case the semileptonic decay branching ratio is 5.3% for the D^0 and the mixing between D^0 and $\bar{D}^0$ is small (<.006 experimentally[24] and estimated theoretically[20,21] to be between 10^{-4} and 10^{-7}). Taking the largest theoretical rate and assuming that we have the same acceptance (25%) for the background dimuons as for the mixing dimuons, we would expect to see a same sign background of 60 to 770 like sign dimuons from $D^0\bar{D}^0$ mixing even if the charm cross section is 1000 times as large as the beauty cross section at 800 GeV/c.

The third background to $B\bar{B}$ mixing that we have considered is produced when one of the B's decays semileptonically and the other B decays nonleptonically. Then if one of the pion decay products of the second B decay itself decays into $\mu\nu$, a same sign background can be produced. Approximately 1% of the beauty decays produces a muon via $\pi\rightarrow\mu\nu$ so that we would expect 30 to 340 same sign background events from this source.

We have examined the possibility that we can further suppress these backgrounds (especially the "daughter" background) by cutting to the high mass μ pairs which should be relatively rich in the muons from beauty decay. Using the $B\bar{B}$ production model of appendix B, we have generated the like sign dimuon mass spectrum for the $B\bar{B}$ mixing signal and for each of the three backgrounds mentioned above: $B\rightarrow C\rightarrow\mu$, $C\bar{C}$ mixing and $B\rightarrow\pi\rightarrow\mu$. These four dimuon mass spectra are shown in

Beauty Physics in E771
Using Single and Multimuon Triggers

I. Introduction

For some time lepton triggers have been understood[1] to be a potentially important means of rejecting ordinary interactions and selecting $B\overline{B}$ events in hadronic interactions. The primary objective of Fermilab experiment E771[2] is the measurement of beauty production and decay as detected using the muons from B->J/Ψ->$\mu\mu$ decays of the various species of B mesons and hadrons. A second important objective of E771 is the accumulation of additional "tagged" B events by triggering on the single muons from B->μ+x semileptonic decays. This note describes the means by which single and dimuon triggers are implemented in E771 and the expectations for obtaining B events from both sources.

In preparing a dimuon trigger system for E771, it was found that a very fast, economical and efficient way of selecting high mass dimuons was to require two muons as defined by the E771 muon detector and to further require that at least one of the muons have a large p_t. Therefore, the E771 trigger, which is designed along these lines, contains a single muon trigger as a natural component. This single muon trigger is a part of Level I and is capable of operating at rates greater than 10^7 interactions per second. So both single and dimuon triggers are available to E771 without additional electronics, and both types of B decay modes can be used to accumulate B data.

The B->J/Ψ->$\mu\mu$ and the B->μ+x decay modes offer different opportunities to the experimentalist. The B->J/Ψ->$\mu\mu$ events are relatively rare but very distinctive. The dimuons from B->J/Ψ->$\mu\mu$ decays are one of the most striking manifestation of beauty production in hadronic interactions and serve as the most powerful method to separate the beauty events from the rest of the total cross section in the offline data analysis. The trigger strategy that E771 has adopted takes advantage of the special attributes of the B->J/Ψ->$\mu\mu$ decays to produce a trigger with a large online rejection of backgrounds due to decays of π's, K's and charm, yielding an extremely low ratio of triggers to interactions.

In addition, the dimuons act as a starting point for the offline analysis, reducing the amount of reconstruction that must be performed on each recorded event before full reconstruction is attempted. The E771 analysis strategy takes advantage of the special features of the B->J/Ψ->$\mu\mu$ decays to produce a very economical offline analysis process. Finally, the B->J/Ψ signature is distinctive enough to permit excellent offline rejection of backgrounds. The observation of a J/Ψ from a secondary vertex unambiguously insures that an event contains a $B\overline{B}$ pair, rejecting almost all potential backgrounds. Because of the potential for achieving low backgrounds to the B->J/Ψ->$\mu\mu$ modes, we have adopted a strategy of collecting every B->J/Ψ->$\mu\mu$ event possible, operating with relatively loose constraints on the dimuon triggers to insure the largest possible acceptance of dimuons in the J/Ψ mass region.

The B->μ+x semimuonic decays offer different challenges and opportunities. However, two features of the B-> μ+x semileptonic decays are very different from the B->J/Ψ modes and are very important. First, the charge of the muon "tags" the decaying B so that some knowledge is gained about its particle or antiparticle nature. This is potentially important for both mixing and, ultimately, for CP studies. In addition and most importantly, the B->μ+x decays are far more copious than the B->J/Ψ->$\mu\mu$ decays. In events containing a $B\overline{B}$ pair, semimuonic decay will produce a muon approximately 23% of the time and approximately 85% of these muons will have a p_t> 0.8 GeV/c. Muons with p_t this large are quite unusual. Semileptonic decays of pions, kaons and charm produce muons with this magnitude of p_t in less than $3x10^{-4}$ of all 800 GeV/c interactions. Therefore, high p_t muons provide a distinctive signal on which to trigger. Because of the large branching ratio and the resulting large number of B->μ+x decays, the single muon trigger strategy produces a very large enrichment factor (ratio of $B\overline{B}$ events to other logged events) of the data written to tape.

Finally, because there are more B semimuonic decays, more losses can be tolerated in the trigger and analysis schemes. This is quite important in a new experimental situation where the cross sections, branching ratios and efficiencies of the experiment are unknown. However, the techniques for offline rejection of backgrounds to the B semimuonic decay

modes is not as simple as the rejection of backgrounds in the case of the B->J/Ψ modes, since the constraint of a J/Ψ from a secondary vertex is not present. The relationship of the single and dimuon triggers and the the data samples obtained with each type of trigger are discussed below.

II. E771 Trigger Scheme

The E771 trigger, as presently being prepared, depends on the detection of unusual muons at Level I (presence of one or more 6 GeV/c muons in the event, at least one of which has a high p_t), unusual global event characteristics at Level II (detection of several moderate p_t hadrons in the event), and detection of secondary vertices at Level III (algorithm for calculating the probability that the event contains a secondary vertex). The scheme is flexible enough to allow a change of criteria at the various levels if experience indicates that other criteria for rejecting the decay backgrounds are more effective.

Level I is composed of two separate parts, Level IA and Level IB, which operate independently and in parallel. Level IA, developed by Lecce, Pavia and the University of Virginia requires the detection of one or more muons as defined by the triple coincidence of an aligned set of pads in the projective pad geometry of the three layers of Resistive Pad Chambers (RPC), embedded in the steel of the E771 muon detector (See Figure 1). The minimum energy required of a muon to penetrate the E771 muon detector steel and produce a signal in the RPC's is 10 GeV in the central part of the acceptance and 6 GeV at wider angles. The RPC chambers have excellent time resolution (<0.5 ns) and rate characteristics that make them adequate even in the hottest area of the E771 muon chamber at rates greater than 10^7 interactions per second.

The Level IB trigger[3], developed by University of Pennsylvania in collaboration with Lecce, Pavia and UVa, requires at least one muons with a p_t above a minimum threshold. The Level IB trigger is based on the idea that the high p_t muon passes through the spectrometer magnet with only limited deflection and these trajectories can be defined for both inbending muons and outbending muons by coincidences between a limited number of pads in the two

dimensional pad structure of the new tracking chambers of the E771 spectrometer. Figure 2 shows (in plan view) some sample trajectories. The Level IB trigger for high p_t muons is formed from the OR of a large number of four fold coincidence between particular sets of pads in the CC1, CC4 pad chambers and in the RPC layer 1, and particular scintillation counters in the CPX scintillation hodoscope. While there are several million possible coincidences between these detector elements, only coincidences that can be caused by an inbending or outbending muon of p_t greater than a preselected threshold are allowed to generate a Level IB trigger. Both the Level IA and IB triggers are implemented using Programmable Logic Gate Arrays. They are both pipelined, requiring a few hundred nanoseconds to accomplish and are capable of operating at rates greater than 10^7 interactions per second. Both Level IA and Level IB are required before higher levels of trigger are interrogated.

Level II (which will not be implemented for the 1990-91 run of E771) will perform complete online tracking in a few microseconds. The implementation of this trigger will be done with associative or content addressable memories presently being developed by INFN. The application of this technology to E771 Level II will be be accomplished through a joint effort of Lecce and UVa. This level of trigger will increase the rejection of the total cross section by imposing the requirement that several tracks with intermediate p_t be present in the event, thereby increasing the probability that the selected events contain high mass B hadrons. Several existing Monte Carlo studies assure us that large rejection factors can be achieved by this sort of criterion. In addition, this sort of online tracking can be applied to the silicon microstrip detector to detect secondary vertices. Once again, existing Monte Carlo studies assure us that large reduction factors in trigger rate can be achieved by the application of this technique to the problem of detecting secondary vertices in an event. These extra rejection factors by Level II online tracking should permit us to increase the rate capability of the E771 experiment toward our ultimate goal of logging all single and dimuon triggers at rates greater than 10^7 interactions per second.

Level III of the E771 trigger system is constructed from several VME based ACP I or II microprocessor modules. We have developed a fast filter program which uses the E771

silicon vertex detector data to search for evidence of secondary vertices. Using relatively simple coding, the filter can, in less than 30 ms, calculate the probability that an event contains a secondary vertex. This detection of a secondary vertex is completely independent of the single and dimuon requirements imposed on the events and, therefore, permits a cut completely orthogonal to the muon criteria.

The effectiveness of this secondary vertex detection algorithm has been extensively studied by a Monte Carlo containing random noise, multiple scattering, gamma conversions, delta ray production and secondary interactions. Rejections factors (shown in figure 3) can range from a few to several tens depending on the efficiency for retaining the beauty signal that is desired. At present we are opting for good efficiency (greater than 90%) and relatively modest rejection factors (approximately 3). No attempt is presently made at any trigger level to require online that the single or double muon be produced at a secondary vertex.

Events passing the software filter are logged by six Exabyte tape units coupled directly to the VME/ACP system. The slowest device in the E771 DA system is presently the 4290 CAMAC TDC's which require 400 μseconds for digitization and readout. Setting the limit on the desirable dead time of the experiment DA to be 25%, results in a limit of 600 events per second of spill, 450 of which can be recorded. Therefore, the overall data recording capacity of the E771 system is presently sized to handle 450 events per second of spill (approximately 125 Mbytes per spill assuming 23 seconds of spill and an E771 event size of 12 Kbytes). Assuming the spill cycle to be 23 seconds of spill out of every 56 seconds of calendar time (similar to the slow spill cycle during the last Fermilab fixed target run), approximately 60% of the data accumulated during the spill will be stored and written to tape in the 33 seconds interspill interval. The remaining 40% will be written to tape during the spill. The storage capacity required of the VME/ACP system for this task is approximately 75 Mbytes and resides in the "Baumbaugh" buffers of the front end of the E771 VME/ACP system. The present plans for the E771 DA are to use Exabyte tapes for data logging. A reasonable assumption for the present generation of tape units is a writing speed of 200 Kbytes per second in the E771 environment. Since 125 Mbytes must be logged every

56 seconds and each tape unit can write 11 Mbytes per 55 seconds of operation, approximately 11 Exabyte tape units are required if no filtering is done at Level III. If the Level III filter performs as advertised, only 6 Exabyte tapes will be required to provide the necessary data logging capability .

III. Expected Performance of the E771 Trigger System

Since we will only have Levels IA, IB and III operational during the first run of E771, we will concentrate on their expected performance for single and dimuons. The vast majority of the raw muon trigger rate is due to the decays of charged pions and kaons. Only at the higher levels of the trigger, can the presence of charm decays in the data can be detected. Using measurements made during E705 and a variety of Monte Carlo's containing π,K and charm semimuonic decays, we have estimated the trigger rates at each level of the trigger. These trigger rates per interactions are shown in Table I below:

Table I
Expected Trigger Rates
per Interaction

Trigger Level	DiMuon Trigger Rates	Single Muon Trigger Rates
IA	$O(10^{-3})$	4×10^{-2}
IB	2×10^{-1}	2.5×10^{-2} *
IA*IB	$O(2 \times 10^{-4})$	10^{-3}
III	.3	.3
IA*IB*III	$O(10^{-4})$	3×10^{-4}

* Achieved by exclusion of outbenders with poor p_t resolution

At an interaction rate of $2x10^6$/second (planned operating point for the 1990-91 E771 run), we expect 400 dimuon and 1000 single muon triggers per second of spill to be present entering Level III. This dimuon trigger rate could conceivably be greater if contributions due to clutter in the RPC's from the 800-900 GeV beam dump or from the beam halos are greater than expected. The total trigger rate of 1400 per second clearly exceeds the present capabilities of the E771 (600 events per second of spill with a dead time of 25%). In fact, the dimuon trigger rate is close to the saturation of the capacity of the data acquisition system. This is not surprising since our trigger system and DA were configured for the expected dimuon rates at $2x10^6$ interactions per second.

Giving priority to accepting the 400 dimuon triggers per spill second generated at $2x10^6$ interactions per second, we presently anticipate the need to reduce the single muon trigger rate to 200 per second. Unless we operate at less than $2x10^6$ interactions per second, we will be able to take a larger fraction of the single muon triggers only if we find ways to improve our single and dimuon triggers or increase our data logging capability. The fraction of single muon triggers that we will be able to record will obviously depend on all these factors and will be uncertain until some experimental experience is gained. However, given that we expect to be able to accept only a fraction of the single muon events at present, we plan to make that fraction of the single muon triggers as rich as possible in B events by concentrating on regions of our acceptance and types of muons where the signal to background at the trigger level is optimal.

The large single muon trigger rate will be tailored to fit into to any residual data acquisition capability in the following ways:

1. By accepting only inbending single muons whose p_t is determined with better resolution than comparable outbenders

2. By limiting the acceptance of the single muon trigger to regions which are relatively rich in B events but where background muons from π and K decays

are smaller (large angle regions).

3. By prescaling the single muon rate to fit the residual data acquisition capacity.

Option 3 is a last resort if we cannot find more discriminating ways to eliminate trigger rate. While we will lose signal using options 1 and 2, our recorded triggers will be richer in B decays. Since the B->μ decays are so copious, we will, for the present, adopt a strategy of being selective about the acceptance and type of single muon events to collect only that portion of the signal where the backgrounds are small and muon p_t resolutions are good. From our Monte Carlo's, we estimate that reducing the solid angle coverage of the single muon triggers to the most favorable 20% to 25%, the trigger rate would be reduced by a factor of 5 while the signal would be reduced by a factor of 3. We also plan to to exclude outbending muons whose p_t resolution is poor from the trigger for the time being.

Taking into account, the 25% dead time of the DA at our nominal operating point of $2x10^6$ interactions per second we will, therefore, be able to process 300 dimuon triggers and 150 single muon triggers per second of spill. Assuming that the Level III filter performs as expected (suppression of the single and dimuon trigger rates by a factor of 3 with 90% efficiency for accepting B->J/Ψ->$\mu\mu$ and B->μ+x), we will log one third of these triggers on tape, leading to a rate of 100 dimuon and 50 single muons triggers per second of spill written to tape.

IV. Estimated Acceptances/Efficiencies of Single and Dimuon Trigger and Offline Analysis

The yields of B decays depend on the geometric acceptances and on the efficiencies of the various elements of the E771 spectrometer and the way they enter into both the trigger and in the offline reconstruction sequence. In addition, the effective cuts required to improve the signal to noise produces some loss of signal as well as a diminution of background. In Table II below, the cumulative effect of the all the acceptances, efficiencies and cuts on the muons from B->J/Ψ->$\mu\mu$ and B->μ+x decays have been estimated using Monte Carlo's, test

beam data for various detectors and the experiences of E705.

The geometric acceptances in Table II - line 1 are calculated using PYTHIA for a mixture of B->J/Ψ->$\mu\mu$ modes. The semileptonic inclusive B->μ+x are generated using the model for fragmentation and hadronization incorporated in PYTHIA. These muons are required to be in the acceptance of the spectrometer and to have sufficient energy to penetrate the various thicknesses of muon steel. As indicated, 40% of the B->J/Ψ->$\mu\mu$ and 67% of the B->μ+x semileptonic decays satisfy this basic requirement.

The efficiency of the Level I trigger for detecting these muons depends critically on the efficiencies of both the resistive plate counters (RPC's) embedded in the muon steel and the PWC pad chambers downstream of the E771 analysis magnet. The efficiencies for the RPC chambers have been determined as a function of rate by E771 in a beam test at CERN in the fall of 1988. The efficiency of the RPC's was found in these tests to be greater than 95% at 50 μ/cm^2/second. This would be highest rate expected anywhere in the RPC's (specifically in the region of the RPC's near the beam when E771 operates at 10^7 interactions per second). For purposes of calculating the trigger efficiency, we have taken an overall RPC efficiency of 95% for the entire muon detector acceptance.

In the case of the PWC pad chambers we have anticipated the problem of vulnerability of the trigger to the efficiency of the chamber by constructing the chamber so that each pad signal is formed from the OR of two identical pads built into the structure of the chamber. Each has its separate gas volume and covers the same solid angle so that there are effectively two chances to pick up the muon tracks. In this way we expect to be able to obtain efficiencies that will be higher for both devices than 95% per plane, the number used in estimating the trigger efficiencies. Since the efficiencies for single and dimuons are high powers of the individual efficiencies (dimuon trigger efficiency = $Eff_{RPC}^6 * Eff_{CC}^2$ and single muon trigger efficiency = $Eff_{RPC}^3 * Eff_{CC}^2$), it is necessary to achieve this level of efficiency for the RPC and PWC pad chambers in order to have a suitably efficient trigger. Our estimates for Level I calculated in this way are shown in Table II-line 2.

The Level IB trigger has two different cuts that are applied to the muon tracks. The first cut, listed in Table II is the minimum pt requirement. For the dimuon trigger this cut is set low (p_t>0.8 GeV/c) in order to maximize acceptance of these relatively rare B->J/Ψ->$\mu\mu$ events. The single muon pt cut is set somewhat higher (p_t>1.0 GeV/c). In addition, only a portion of the relatively poor pt resolution outbenders are accepted in the single muon triggers. Taking into account all acceptances, detector efficiencies and Level IB cuts, the cumulative efficiency for the muon part of the trigger is estimated to be 25% for dimuons and 23% for single muons.

The Level III cuts have been exhaustively estimated as described above by an extensive Monte Carlo. The silicon vertex detector information is used to calculate, exploiting a simple algorithm[4] which depends on a function of the impact parameters of all tracks in the event, a quantity related to the probability that the event has no secondary vertex. The distribution of this quantity is strikingly different for B events containing secondary vertices and events containing only a primary vertex. This quantity can be used to select events containing B's as shown in figure 3. We presently plan to set cuts so that >90% of the B's are retained.

In the case of the offline analysis, we have extrapolated from the E705 experience reconstructing muons, taking into account the improvements that we anticipate in E771. We have estimated the vertex cut efficiencies for single muons using the Monte Carlo's mentioned above which were used to test the algorithm for Level III secondary vertex detection. As mentioned above, these Monte Carlo's include random noise, multiple scattering, gamma conversations, delta ray production and secondary interactions. The offline reconstruction and vertex cuts outlined in the offline strategies discussed below will lead to efficiencies for the muon part of the event listed in Table II.

Finally, the overall cumulative efficiency for passing the muons from B->J/Ψ->$\mu\mu$ and B->μ+x through the trigger and analysis chain is approximately 9% for both channels. The efficiency for the rest of the decay products must be estimated on a mode by mode basis.

Table II

B->J/Ψ->μμ and B->μ+x

Muon Acceptances and Efficiencies

	B->J/Ψ->μμ	B->μ+x
Geometric Acceptance for Muon Triggers	0.4	0.67
Level I Trigger efficiency due to detector efficiencies	0.66	0.77
Level IB P_t cut efficiency for muons	>0.95	0.67
Level IB muon outbender cut	-	0.67
Cumulative Level I trigger acceptance/efficiency	0.25	0.23
Level III Secondary Vertex Algorithm Efficiency*	0.9	0.9
Offline reconstruction efficiency for muons	0.8	0.9
Offline Vertex cut requirements for muons	0.5	0.5
Cumulative offline muon efficiency	0.4	0.45
Composite Acceptance/Efficiency for single or dimuons	0.09	0.09

*Level III does not involve muons

V. Comparison of the B->J/Ψ->μμ and B->μ+x Data Samples

Certain features of the two types of B data samples have already been mentioned earlier in this note. We estimate below the richness of the two different trigger samples in B

decays and the signal to background that we expect at each level of the trigger and off line analysis, using the expectation that $1/1.5 \times 10^6$ of all interactions will contain B's.

V.a B->J/Ψ->μμ Data Sample

Because of the cumulative branching ratios, the portion of the dimuon triggers due to actual B decays is relatively small. Given the 1.1% branching ratio for B->J/Ψ + anything and the 6.9% branching ratio for J/Ψ->μμ, only 1.5×10^{-3} of the BB events will be collected by the dimuon trigger strategy (taking into account that there are two B's in every event). Therefore, only one event out of every 10^9 interactions will have a B->J/Ψ->μμ decay.

However, the backgrounds to the B->J/Ψ->μμ events can reduced more easily in the trigger and the offline analysis than the backgrounds to B->μ+x events, since the constraint of requiring J/Ψ's at secondary vertices is very powerful. The requirement for the dimuon to be a J/Ψ, by itself, eliminates a large portion of the background decay dimuons. For 800 GeV/c p Si interactions the J/Ψ production cross section is estimated to be approximately 11μb (using an A dependence of $A^{0.93}$). The $B\overline{B}$ beauty hadron production cross section in an 800 GeV/c p Si interactions is estimated to be approximately 280 nb assuming a linear A dependence of the beauty production cross sections and using the third order beauty hadroproduction cross section calculations of K. Ellis. Using a branching ratio for B->J/Ψ of 1.1 % , we estimate that 1/1800 of the produced J/Ψ's are due to a $B\overline{B}$ event in which one or the other of the B's decayed via a J/Ψ decay mode. Therefore, the first objective of the online trigger and the offline analysis will be to select events containing J/Ψ->μμ decays. Taking into account that the direct J/Ψ production is decreased by a factor of three by the vertex requirements of the Level III algorithm (as are the π, K decay backgrounds), we expect that 1/600 J/Ψ entering the online analysis stream will be due to a B decay. Approximately 90% of the B events survive Level III.

A second offline condition that can be applied after the J/Ψ signal is obtained is to require that the muon pair from the J/Ψ decay comes from a secondary vertex. The vertex

cuts necessary to impose this condition are estimated to lose approximately 50% of the signal but make a further dramatic improvement in the signal to background ratio (greater than a 1000 from our Monte Carlo). This improves the signal to background ratio to better than 1/1 for B->J/Ψ. Finally, detection of at least one additional track from the candidate secondary vertex will further reduce the probability that the event is a mismeasured J/Ψ by a factor greater than 10, leading to signal to background ratio greater than 10/1. Since the invariant masses of the remaining background events are spread over a large kinematic range, there will be essentially no backgrounds to the reconstructed B->J/Ψ mass spectra for specific exclusive final states.

V.b B->μ+x

In contrast to the small cumulative branching ratio for B->J/Ψ->$\mu\mu$, approximately 23% of all BB events will produce at least one muon via the semileptonic decay modes and that muon will have a high p_t a large fraction of the time (67% for p_t >1.0 GeV/c). This difference in branching ratios will allow a much greater number of B->μ+x events to be produced for a given number of interactions as shown below in Table III.

The trigger strategy for obtaining the single muon trigger sample proceeds along lines similar to those of the dimuon triggers. In spite of the fact that the B->μ decays are less distinctive than the B->J/Ψ->$\mu\mu$ decays, the percentage of events passing trigger level I containing a B->μ+x is still much greater than the fraction which contain B->J/Ψ->$\mu\mu$ decays because of the large branching ratio for B->μ+x. An enrichment factor of one $B\overline{B}$ event for every 6000 triggers is obtained for the single muon trigger sample written to tape, as compared to 1/370,000 for dimuon triggers. Thus, as we shall see in Section VI, in our short 1990-91 run, we may be able to record as many as 15 K B->μ+x events on tape.

The first step of B->μ+x offline analysis increases the B->μ+x enrichment factor to 1/1200 by sharpening the resolution of the p_t cut made on the completely reconstructed muon. The second step in the offline analysis for all single muon triggers is to require that the muon not come from the primary vertex. According to Monte Carlo studies, the

requirement of a 30 micron impact parameter for the muon in the E771 silicon microvertex detector improves the signal to background by a factor of approximately 10, producing an enrichment factor of 1/120 events while retaining approximately 50% of the signal. Finally, finding additional charged tracks which are part of the secondary vertex, will help to eliminate false secondary vertex single muon candidates due to mismeasured single muons. The detection of additional tracks from the secondary vertex reduces the backgrounds by a factor greater than ten leading to a signal to noise in the resulting data sample of greater than 1/12.

Several additional strategies can be employed to further isolate a sample of events containing B's before complete reconstruction is attempted. These strategies will depend on whether the objective is to reconstruct the semileptonic B decay (by means of a zero c fit) or to reconstruct the other B in the event (which can decay into any one of a number of different modes). In both cases, simple examination of the overall topology of the event may help determine if the event contains a $B\overline{B}$. For example, $B\overline{B}$ events can be further distinguished from the charm and other backgrounds by stratagems such as the observation of tertiary vertices. Another stratagem that is possible without complete reconstruction of the event is the determination that the invariant mass of a part of the secondary vertex decay products have mass greater than the charm mass. Depending on the mode, these sorts of strategies may help to select a sample of events with a higher probability for containing a $B\overline{B}$.

Since the final signal to background ratio will depend on the branching ratios, acceptances and efficiencies for sought after decays, as well as the rejections of the specific backgrounds to those decays, we do not attempt to define a global strategy because of the many, as yet unknown, parameters. However, if we can reach a signal to background of one $B\overline{B}$ event for every 10-20 background events, then, because of the wide range of masses of the reconstructed background secondary vertices, we will be able to search with good sensitivity for the presence of B mesons in various final states with very small backgrounds to the reconstructed B mass peaks.

Table III

Enrichment Factors at Various Levels

Level	DiMuon Trigger (signal = B->J/Ψ->$\mu\mu$)	Single Muon Trigger (signal = B->μ +x)
BB/ interaction	$1/1.5x10^6$	$1/1.5x10^6$
signal/interaction	$1/10^9$	$1/6.5x10^6$
signal/ IA*IB trigger	$1/8x10^5$	$1/2.8x10^4$
signal/ tape event	$1/3.0x10^5$	$1/6x10^3$
Offline Step I Signal/background*	$1/6x10^2$	$1/1.2x10^3$
Offline Step II Signal/background	>1/1	$1/1.2x10^2$
Offline Step III Signal/background	>10/1	>1/12

*Assumes a factor of three reduction of the directly produced J/Ψ due to Level III filtering versus a retention of 90% of the B->J/Ψ->$\mu\mu$ signal.

VI. 1990-91 Run Estimated B->J/Ψ->$\mu\mu$ and B->μ+x Yields

Given the present schedule for E771, we can, at best, expect approximately three months of data logging, beginning early in 1991. Assuming three months of operation (12 weeks at 100 hours per week with a 23 seconds of spill out of every 56 seconds of spill = 1.8 $x10^6$ seconds of spill) at 2 $x10^6$ interactions per second, the E771 spectrometer will sample 3.6 $x10^{12}$ 800 GeV/c p Si interactions. $2.4x10^6$ $B\overline{B}$ events will be produced in that short period and $2.7x10^8$ events will be recorded on tape. Table IV below summarizes the yield of B->J/Ψ and B->μ+x at the major junctures of the data processing.

Table IV

Estimated B Yields, 1990-91 Run

(Est. 1.8 x 10^6 seconds of spill)

	$B->J/\Psi->\mu\mu$	$B->\mu+x$
Signal Produced	3.6 $x10^3$	5.5 $x10^5$
Signal on Tape*	6.0 $x10^2$	1.5 $x10^4$
Signal surviving offline analysis*	2.6$x10^2$	6.8 $x10^3$

*The offline analysis referred to is the first two steps which deal only with the muons from the B decay. The number for $B->\mu+x$ includes reducing the single muon triggers by a factor of 5 as discussed on page 8 to fit into the present DA capability of E771.

As shown in Table IV, the first short run of E771 can result in the accumulation of a few hundred $B->J/\Psi->\mu\mu$ events on tape some of which can be totally reconstructed. Given the efficiencies/acceptances for the decay products other than the muon and the measured or expected branching ratios for various exclusive decay modes such as $B->J/\Psi\ K^0_S$, we might expect to be able to reconstruct a few events in each of several exclusive mode. There would be almost no background to these events.

In addition, we can accumulate more than 15K $B->\mu+x$ decays to be written to tape in the short 1990-91 run even under the constraint of being very selective of the single muon triggers. Of the logged single muon triggers, 9 K will survive the muon part of the analysis sequence. This data should include appreciable numbers of events in several exclusive decay modes in which the decay products of the "other" B are in the acceptance of the spectrometer and can be totally reconstructed. An example of such decay modes are the $B->D^*$ decays some of which which have mainly charged decay products and have reasonable acceptances and branching ratios.

VII. 1992-93 Run Estimated B->J/Ψ->μμ and B->μ+x Yields

The short run in 1990 should allow us to understand our triggers, tune our spectrometer and collect some data. However, we plan for operations at a much higher rate in the 1992 run, nominally operating at 10^7 interactions/second or greater. Our Level II trigger, presently under development, will allow us to accommodate these higher rates, to accumulate the bulk of both the single and dimuon triggers produced in the 1992-93 run. In addition, to be able to operate at the higher rates, some improvements must be made in the rate capability of certain components of our spectrometer (in particular the central region of the EM detector). Finally, we propose to add for the 1992 run a Cerenkov for K, π, and p identification to the spectrometer to allow complete reconstruction of B events with K's or proton decay products.

With these improvements and assuming the 1992 fixed target run is ten to eleven months long (the approximate total length of the 1990-91 run), operation at 10^7 interactions per second for eight months during that run will result in approximately 4.8×10^6 seconds of spill delivered to E771, resulting in 4.8×10^{13} interactions sampled by the spectrometer. If we can operate at 10^7 interactions per second in the 1992-93 run, 3.2×10^7 $B\bar{B}$'s will be produced and 7.2×10^8 events will be written on tape (assuming no increase in the E771 data acquisiton system capabilities will be required, in addition to our trigger improvements, to accommodate the increased operating rate). Table V below shows the expected yields of B->J/Ψ->μμ and B->μ+x under these assumptions:

Table V

Estimated B Yields, 1992-93 Run

(Est. 4.8×10^6 seconds of beam)

	B->J/Ψ->μμ	B->μ+x
Signal Produced	4.8×10^4	7.4×10^6
Signal on Tape*	6.4×10^3	1.1×10^{86}
Signal surviving offline analysis*	2.6×10^3	5.0×10^5

*Assumes that no prescaling or strong selection of single muon triggers is necessary in 1992. Assumes that the E771 trigger system is improved to accommodate all the single and dimuon triggers at 10^7 interactions per spill second.

VIII. Computing Requirements of E771

Given the E771 capacity for logged on tape, we can estimate the requirements for offline computing for the fall, 1990 run of E771 and for the 1992 run assuming that the E771 data acquisition capability remains at 600 events per spill second during that period (450 events per spill second logged to tape). Based on this assumption, the expected accumulation of events on tape during those two runs is approximately 10^9 events, given our ability to filter at Level III to match the tape writing capabilities of six Exabyte units.

The E771 concentration on muon signatures for B events gives a focus to the offline analysis. Because of this considerably less computer time is needed per event than for experiments which must search globally for evidences of secondary vertices and do complete reconstruction to determine if a secondary vertex is due to a B decay. The muon based B analysis strategies allow structuring of the analysis programs to filter with successively more and more sophistication with the number of remaining events decreasing dramatically at each stage. For purposes of estimating the computing time required for the analysis, we have assumed a mixture of single and dimuon triggers with the 1990-91 data dominated by dimuon triggers and the 1992-93 data weighted toward single muons (presuming that we can find improvements of the triggers such that the logged events will tend toward the more natural split between single and dimuon triggers of 3 to 1.

Considering first the data we might hope to obtain in the 1990-91 run, we estimate first the computing requirements for $B \to J/\Psi \to \mu\mu$ decays (1.8×10^8 triggers on tape). We will express the needs of the various analyses in units of VAX780 years. A year will be taken to be 10^7 seconds for purposes of these estimates (Computing duty factor of 1/3).

The stages in the dimuon offline data analysis process are:

1. The first step will be a fast filter program to determine if the dimuon has a mass greater than 2.5 GeV/c^2. This filter will select events containing J/Ψ's or determine if both muons have a p_t greater than 1.0 Gev/c (to select events in which both B's have decayed semileptonically). Based on our E705 experience, such a filter program, computing a relatively crude dimuon mass, can reduce the data sample by a factor of 5 at a rate of 250 ms per event on a VAX780. The pad structure of the new E771 chamber set should allow us to achieve a larger rejection factor in less time per event. Using the E705 experience as an upper limit, the total computer time required to perform this first step for the 1990-91 data (assuming $2x10^8$ dimuon triggers on tape) would be, approximately 5 VAX780 years, passing less than $4x10^7$ events on to subsequent analysis steps.

2. The second step in the offline analysis of the dimuon will be a second pass, higher resolution, three dimensional reconstruction of the dimuons. This step is estimated to take considerably less than the 3 VAX780 seconds per event that required for an E705 event since the pad chambers in E771 should greatly speed up three dimensional track finding. In any case, using the E705 experience as an upper limit, we estimate approximately 10 VAX780 years to accomplish this step and a reduction of the data sample by a factor of 20, leaving 2 million dimuon candidate events for further analysis. Moreover only a few hundred thousand of these will be contained in the J/Ψ mass region.

3. A third step in the analysis process will be a filter program which checks the muon tracks to determine if they come from secondary vertices. The program which uses the three dimensional high p_t muon track found in the spectrometer chambers in step 2, extrapolates the track back into the silicon vertex detector. In this way, the process of finding the muon track in the silicon vertex detector can be greatly speeded up since not all silicon hits need be involved in the silicon muon track finding process. The silicon muon track, found in this way, is checked to see if it comes from the primary vertex (defined at this stage as being the intersection of a target foil and a beam track as reconstructed from

the beam silicon tracker). This process, which should be relatively fast (estimated to be less than 500 ms per event or less than a VAX780 year), would filter the dimuon data by a factor much greater than 10, reducing the data sample to a few hundred thousand for the final analysis step.

4. The final stage in the process is an analysis of the remaining events in some detail to isolate and separate the final data sample of B decays. It is not unreasonable to imagine that the remaining process would be quite lengthy since we will have to completely reconstruct all tracks, including the electromagnetic signals. Since we have no experience to draw on, we will assume 30 VAX780 seconds per event as an initial estimate for this final step of extracting the B signals from these few hundred thousand events. This would result in less than a VAX 780 year to complete the process of extraction of the signal.

The single muon analysis scheme is similar to and is intermingled with the analysis stream for the dimuons.

1. The first step for single muons would be a part of the first step filter program for dimuons. There will be a relatively crude check of the high p_t trigger muon with better resolution than is possible with the online trigger. We estimate that a factor of 4-5 rejection will still be possible at this step for single muon triggers given that we will apply tighter cuts to the single muon sample. Assuming a data sample of 10^8 single muon triggers, approximately $2x10^7$ events will pass on to later stages of analysis. Approximately 3 VAX780 years will be required for this step for the 1990-91 single muon data sample.

2. The second step in the analysis tree for single muons is also similar to that of the dimuon analysis. We plan to reconstruct the single muon completely and apply more restrictive quality criteria to it than have been applied in step 1 filter. However, because we do not have the constraint of the J/Ψ mass, we will not realize as great a reduction factor from this step as we can obtain in the dimuon trigger data. We estimate a factor of three rejection of background in this step, leaving $7x10^6$ events for the third level of the analysis. This step is estimated to require 6 VAX780 years for the single muon trigger

sample from the 1990-91 run.

3. The third step in the analysis process is similar to the third step in the analysis of the dimuons. However, this filter is much more important for the single muon trigger than for dimuon triggers since the second step of the single muon analysis is not as powerful as the second step of the dimuon analysis. This filter will require 1.5 VAX780 years for the 7 $x10^6$ single muon triggers in the 1990-91 data, and should filter by a factor of 10, reducing the data sample to less than a million for the final analysis.

4. We anticipate that the extraction of the B signals from the single muon triggers that remain at this stage will be more difficult than the extraction of B's from the J/Ψ sample. In addition we will have approximately 10 times as many events at this step to completely reconstruct. Therefore, we, rather arbitrarily, estimate that this step will require 60 VAX780 seconds per event, leading to 6 VAX years to accomplish this task for the 1990-91 data.

By summing the steps required for the analysis of single and dimuon triggers, we can see that, roughly speaking, we can expect a single trigger to take twice as long to analyze as a dimuon trigger on average, most of the difference coming in our assumptions about the relative weakness of step 2 in the single muon analysis process and the additional difficulties anticipated in the final step of the analysis in extracting the B's from the more background prone single muon triggers. However, the total computing power that needed for all the 1990-91 data is not excessive, totaling less than 40 VAX780 years.

The analysis streams would be approximately the same for the 1992-93 data but we would have many more events to analyze ($7.2x10^9$ compared to $3x10^8$). We also might expect these events to be more dominated by the single muon triggers. Under this worst case scenario, we estimate less than 200 VAX780 node years will be required for the 1992-3 data sample.

In conclusion, while these crude estimates of the computing time required for E771

are the best that can be done at the moment given our lack of experience in the process of analyzing decays in a silicon vertex detector, they are probably not totally out of line with our eventual needs. We have not invoked the power of the new PWC pad chambers in estimating the times required for our level 2 filter and we are probably conservative in estimating the times required for the final step in extracting the B signals. The factors may balance the inexperience and the oversights that are surely present in our present thinking about the E771 analysis procedures.

Table V

E771 Computing Requirements

	1990	1992
Spill Seconds	1.8×10^6	4.8×10^6
Interactions produced	3.6×10^{12}	4.8×10^{13}
BB produced	2.4×10^6	3.2×10^7
Events logged to tape*	2.7×10^8	7.2×10^8
VAX780 node years to process	<40	<200

*Assumes that the trigger effectiveness can be improved by the time of the 1992 run to accommodate the increase in interactions/sec

---

IX . Summary

The ability to trigger on high p_t single muons is an intrinsic part of the E771 dimuon trigger. Having this capability will broaden the ability of E771 to study B decays, giving us an additional option in this, as yet, undeveloped area of experimentation. The single muon triggers are the most copious B signature that can be easily triggered on and produce the largest enrichment factor in the data logged to tape. Exercising this capability will allow us to write several hundred B->J/Ψ->$\mu\mu$ and over 15 thousand B->μ events onto tape in the 1990-91 run and may eventually lead to data samples of several thousand of B->J/Ψ->$\mu\mu$

events and greater than one million B->μ+x on tape in the 1992-93 run. The amount of computing time per single muon trigger trigger required to analyze these events is probably within a factor of two of the time required for dimuon triggers. In any case, the total computing time required for the mixed trigger samples that we expect to accumulate is not excessive by the standards of several charm experiments due to the fact that we have the muons to guide our analysis process.

References

1. B. Cox and D. Wagoner, "The J/Ψ Trigger for Study of Weak Beauty Decays at the SSC", Proceedings of the Summer Study on the Physics of the Superconducting Super Collider, 1986, 83(1986).
2. Fermilab Proposal E771, April 1986.
3. W. Selove, "Steps Toward High-Rate Fixed-Target B Physics", University of Pennsylvania Report UPR-161E, November 1988.
4. M. Cooper and J. Trischuk, E771 Internal note, January, 1990.

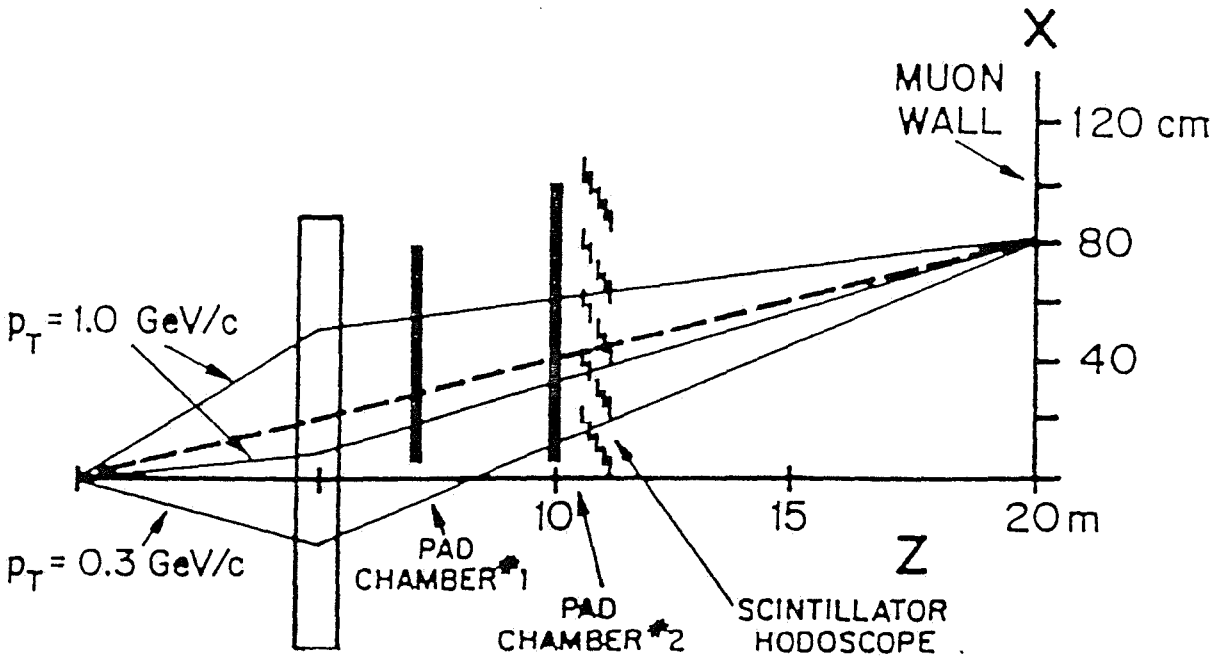
X
MUON
WALL
120 cm
80
40
p_T = 1.0 GeV/c
p_T = 0.3 GeV/c
10
15
20 m
Z
PAD
CHAMBER #1
PAD
CHAMBER #2
SCINTILLATOR
HODOSCOPE

Figure 2

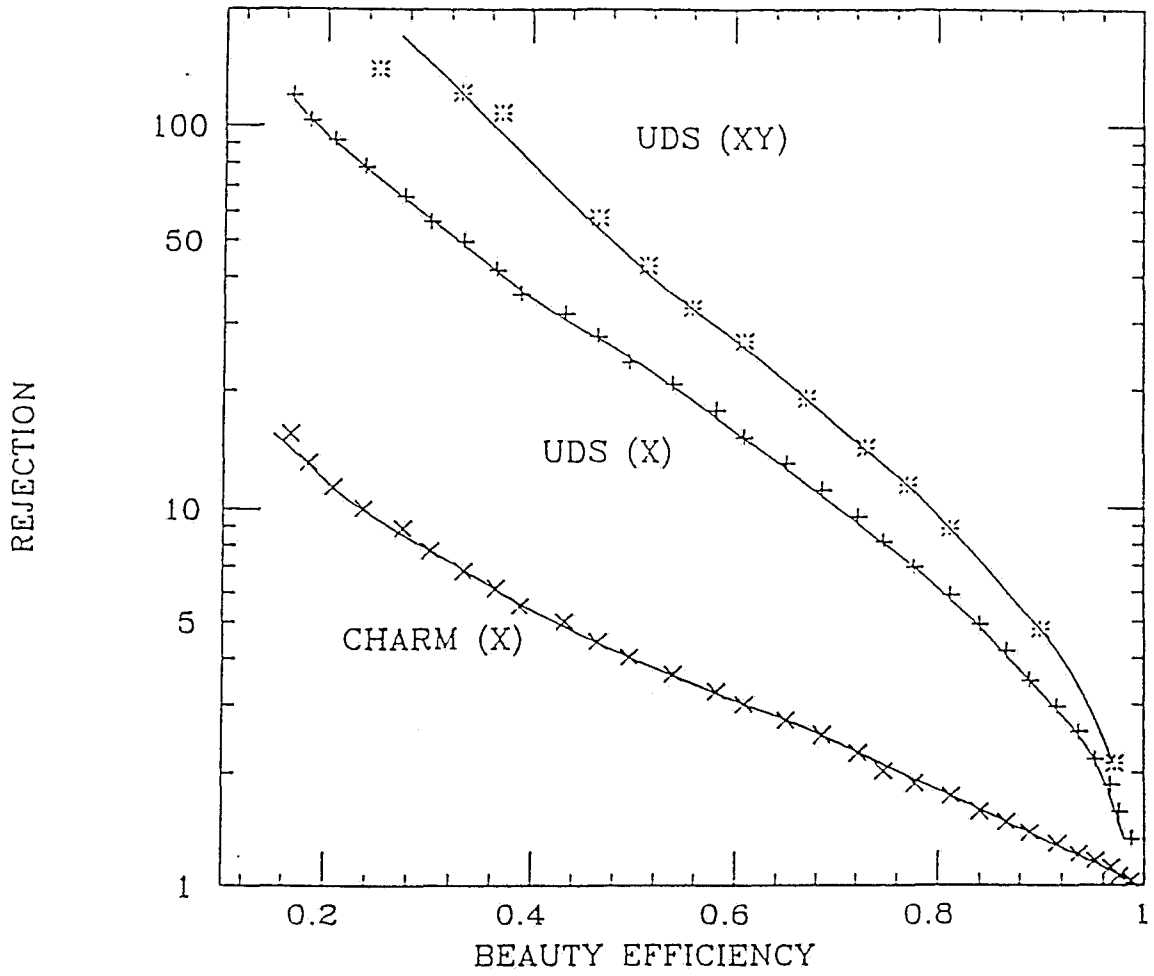
REJECTION vs BEAUTY EFFICIENCY
REJECTION
100
50
10
5
1
UDS (XY)
UDS (X)
CHARM (X)
0.2
0.4
0.6
0.8
1
BEAUTY EFFICIENCY

Figure 3